Electronic Theses and Dissertations   Theses, Dissertations, and Major Papers

1973

Coherence transfer between the (2)P(12)and (2)P(32) resonance states in sodium and potassium, induced in collisions with noble gas atoms simple molecules.

Barbara. Niewitecka
University of Windsor

Follow this and additional works at: https://scholar.uwindsor.ca/etd

COHERENCE TRANSFER BETWEEN THE $^2P_{1/2}$ AND $^2P_{3/2}$

RESONANCE STATES IN SODIUM AND POTASSIUM,

INDUCED IN COLLISIONS WITH

NOBLE GAS ATOMS AND SIMPLE MOLECULES

by

Barbara Niewitecka

A Thesis
Submitted to the Faculty of Graduate Studies through
the Department of Physics in Partial Fulfillment
of the Requirements for the Degree
of Doctor of Philosophy at the
University of Windsor

Windsor, Ontario

1972

ABSTRACT

Transfer of coherence accompanying $^2P_{1/2} \rightarrow {}^2P_{3/2}$
excitation transfer in sodium and potassium, induced in
collisions with inert gas atoms and simple molecules, has
been investigated. Sodium or potassium atoms were excited
by σ^+ polarized D_1 radiation which produced an orientation
in the $^2P_{1/2}$ state. The orientation was then transferred to
the $^2P_{3/2}$ state in collisions with buffer gas atoms or mole-
cules. As a result of the coherence transfer, the observed
sensitized fluorescence emitted in the decay of the $^2P_{3/2}$
atoms, was partly polarized. The dependence of the polari-
zation of the sensitized fluorescence on the strength of the
magnetic field which was perpendicular to the excitation-
observation plane (Hanle effect), was studied with various
noble gases. The widths of the Hanle signals in sensitized
fluorescence appeared independent of the buffer gas pressure
and were found invariant from one gas to another.

The experiments yielded the following values of
$^2P_{1/2} \rightarrow {}^2P_{3/2}$ coherence transfer cross sections. Na-He,
7.1 Å^2; Na-Ne, 6.2 Å^2; Na-Ar, 12.0 Å^2; Na-Kr, 6.8 Å^2;
Na-Xe, 6.9 Å^2; K-He, 1.7 Å^2; K-Ne, 0.8 Å^2; K-Ar, 0.5 Å^2;
K-H_2, 3.5 Å^2; K-CH_4, 7.0 Å^2; and K-CD_4, 7.7 Å^2.

ACKNOWLEDGEMENTS

I am most grateful to Dr. L. Krause, under whose supervision this research was conducted, for his support and encouragement throughout the course of this work.

I wish also to express my gratitude to Dr. M. Elbel for his instruction and supervision during the initial stages of this study, to Dr. M. Czajkowski for many helpful and enlightening discussions, and to Dr. W. Baylis for valuable advice on the theoretical aspects of the problem.

Acknowledgements are due to Master Glassblower Mr. W. Eberhart who produced the fluorescence cells and much of the glass vacuum system, and to Mr. W. Grewe, Machine Shop Superintendent, who manufactured several component parts of the apparatus.

TABLE OF CONTENTS

LIST OF TABLES

LIST OF FIGURES

viii

I. INTRODUCTION

When an alkali atom is optically excited to its $^2P_{1/2}$ resonance state by the absorption of circularly polarized light, it also becomes spatially oriented and the D_1 fluorescence emitted as the result of its decay, is circularly polarized. If, before decaying, the oriented $^2P_{1/2}$ atom collides with a noble gas atom or molecule, the collision will induce mixing between the ^2P states and will also cause depolarization of the resonance fluorescence. Fine structure mixing between ^2P states in sodium and potassium has been studied extensively during recent years and mixing cross sections have been reported for sodium by Pitre and Krause (1967), and Stupavsky and Krause (1969), and for potassium by Chapman and Krause (1966), and McGillis and Krause (1968).

The depolarization of sodium resonance fluorescence induced in collisions with helium, neon and argon atoms was first investigated by Hanle (1927). More recently, several detailed studies of depolarization of alkali resonance fluorescence were carried out using methods such as optical pumping with D_2 light (Franz and Franz, 1966; Franz, 1969; Elbel and Naumann, 1967; Fricke et al, 1967; Ackermann and Weber, 1968; Zhitnikov, Kuleshov and Okunevitch, 1969), Hanle effect (Gallagher, 1967; Tudorache, 1970), and Zeeman scanning techniques (Berdowski, Shiner and Krause, 1971;

1

Guiry and Krause, 1972). Most theoretical treatments of depolarization of excited atoms were based on time-dependent perturbation theory (Byron and Foley, 1964; Callaway and Bauer, 1965; Omont, 1965; Wang and Tomlinson, 1969). Cross sections for depolarization of alkali ^2P states, due to collisions with noble gas atoms, calculated by Grawert (1969); Nikitin and Ovchinnikova (1969), and Elbel (1970), are in good agreement with experimental results.

It might be expected that an additional effect should take place during the collisions, which would result in the transfer of polarization from one ^2P state to the other. Indeed, a calculation of relative probabilities for collision-induced transitions between Zeeman substates of the two ^2P states leads to the conclusion that polarization created in the $P_{1/2}$ state can be transferred to the $P_{3/2}$ state as the result of a single collision. This result may be reached on the basis of the weak collision model (Elbel and Naumann, 1967a,b; Elbel and Schneider, 1968; Wang and Tomlinson, 1969) or of the L-randomization model (Franz and Franz, 1966).

The transfer of polarization may be described in the following qualitative terms. The spin $\vec{S}$ in the $^2P_{1/2}$ state points in the direction opposite to the total angular momentum $\vec{J}$ while the orbital angular momentum $\vec{L}$ points in the same direction as $\vec{J}$. The collision destroys partly or completely the orientation of $\vec{L}$ and its direction becomes random but the orientation of $\vec{S}$ remains unchanged. The

unaffected spin and the disordered angular momentum together represent a mixture of ^2P states which includes the inherent Zeeman substates of the $^2P_{3/2}$ state. These Zeeman substates must be polarized in the same sense as the spin, namely in a direction opposite to the initial orientation of $\vec{J}$ in the $^2P_{1/2}$ state, since in the $P_{3/2}$ state $\vec{S}$ and $\vec{J}$ are parallel to one another.

The assumption that the orientation of $\vec{S}$ remains unchanged is strictly valid only when the collision time is significantly shorter than the period τ_{LS} of spin-orbit precession, which is the case for lithium and sodium. The validity of this assumption for sodium has recently been proved by Schneider's (1971) experiments. For potassium, however, the collision time is approximately equal to τ_{LS} and the L-randomization picture can only be regarded as being of qualitative significance.

The whole situation changes radically in the presence of nuclear spin $\vec{I}$ which is coupled to $\vec{J}$ as the result of hyperfine interaction. In both sodium and potassium $I = 3/2$ and thus the $^2P_{1/2}$ state splits into two h.f.s. states and the $^2P_{3/2}$ into four, causing the appearance of a whole gamut of hyperfine Zeeman substates in the presence of a magnetic field. The nuclear spin remains unaffected by atomic collisions but, as has recently been pointed out by Bulos and Happer (1971) and by Papp and Franz (1972), hyperfine interaction may reorient the nuclear spin during the time τ_c between two consecutive collisions. The significance of

this effect can be estimated by comparing with τ_c the I-J precession period τ_{hf} (which corresponds to the inverse of the energy gap between adjacent hyperfine states). If $\tau_c \ll \tau_{hf}$, nuclear orientation does not change between collisions. From kinetic theory of gases,

$$(1) \qquad \tau_c = \frac{1}{4} \sqrt{\frac{\pi}{2}} \quad \frac{1}{N \pi r^2 v_r} \quad,$$

where N ($\simeq 10^{15}$ cm^{-3} at 1 torr) is the density of the buffer gas, πr^2 is the depolarization cross section which is of the order of 100 Å^2 for alkali-noble gas atomic collisions (Elbel and Schneider, 1968; Berdowski, Shiner and Krause, 1971), $v_r = \sqrt{8kT/\pi \mu} \simeq 10^5$ cm/s is the average relative speed of the colliding partners, μ is their reduced mass, k is the Boltzmann constant and T is the absolute temperature. It may be inferred from the values τ_{hf} and τ_c which are listed in Table I, that nuclear spin effects can be disregarded in potassium-buffer gas collisions because in potassium τ_{hf} is about one order of magnitude larger than τ_c. In sodium $\tau_c \simeq 1/2 \, \tau_{hf}$ and nuclear spin may be partly disoriented between two consecutive collisions.

The transfer of polarization in atomic collisions was first observed by Gough (1967) who detected it in collisions between aligned $6\,^3P_1$ mercury atoms and $5\,^1S_0$ ground-state cadmium atoms. The implications of Gough's results were discussed by Series (1967) who also pointed out that the transfer of polarization between atomic states amounts to a transfer of coherence which had been created in

TABLE I

H.f.s. Splittings, τ_{hf}, τ_c and Natural Lifetimes
of ^2P States in Sodium and Potassium

	$\triangle E_{hf}$ (appr.)	$\tau_{hf} = \dfrac{1}{\triangle E_{hf}}$	τ_c	τ Natural Lifetime
$^{23}Na(^2P_{1/2})$	95 MHz [d]	1×10^{-8} s		1.6×10^{-8} s [a]
$^{23}Na(^2P_{3/2})$	30 MHz [c]	3×10^{-8} s	1.4×10^{-8} s	
$^{39}K(^2P_{1/2})$	29 MHz [d]	3×10^{-8} s		2.77×10^{-8} s [b]
$^{39}K(^2P_{3/2})$	10 MHz [c]	1×10^{-7} s	1.3×10^{-8} s	

(a) Kibble, Copley and Krause (1967)

(b) Copley and Krause (1969)

(c) Schmieder et al (1970)

(d) approximate values

the primarily excited state by exciting the atoms with polarized light. Gough found that the polarization of the sensitized fluorescence emitted by the collisionally excited Cd 5^3P_1 atoms was 2%-5%. Cheron and Barrat (1968) interpreted Gough's results using density matrix formalism as well as a "selection rule" for atomic collisions, which had been proposed by Franzen (1959) and which states that the sum of the J_z components along the collision axis must be conserved.

Sametis and Kraulinya (1969) similarly observed transfer of alignment and of orientation in mercury-thallium collisions, with the thallium sensitized fluorescence being circularly polarized to the extent of about 5% (Kraulinya, Sametis and Bryukhovetskii, 1970). More recently, the transfer of polarization in the course of Penning ionizing collisions between helium and strontium atoms was observed by Schearer and Riseberg (1971).

A theoretical study of collisional coherence transfer has been reported by Chiu (1972), who in his calculations considered a pure electric dipole-dipole interaction as being responsible for both excitation and coherence transfer. According to Chiu, the polarization of sensitized fluorescence should depend only on the angular momenta of the atomic states between which coherence is being transferred, but should be independent of the relative velocity of the colliding partners and of ΔE, the energy gap across which coherence is transferred.

In contrast to the cases were polarization is

collisionally transferred from one atomic species to another, it is also worthwhile to consider the situation where coherence is being retained within the same atomic species during its collisional transfer from one excited state to another. Such an effect in sodium has been demonstrated by Elbel, Niewitecka and Krause (1970) who studied coherence transfer from the $3^2P_{1/2}$ to the $3^2P_{3/2}$ state. The cross sections for such transfer of polarization were determined by Elbel and Schneider (1971).

Investigations of coherence transfer in sensitizing collisions between excited alkali atoms and buffer gases contribute to the understanding of the mechanism responsible for the process of excitation transfer. The aim of the present investigation is to study the transfer of coherence accompanying the transfer of excitation between $^2P_{1/2}$ and $^2P_{3/2}$ resonance states in sodium and in potassium, induced in collisions between the excited sodium or potassium atoms and noble gas atoms or simple molecules, and to explore the interrelationship between the phenomena of disorientation, coherence transfer and fine-structure mixing.

II. THEORETICAL

The variation of resonance fluorescent intensity with magnetic field strength was first investigated by Hanle (1927) who arranged his experiment as shown in Fig. 1. A beam of mercury 2537 Å resonance radiation, linearly polarized at right-angles to the direction of a magnetic field $\vec{H}$ pointing along Oz, was made incident on mercury vapour contained in a fluorescence cell. The emitted resonance fluorescence was detected in the direction parallel to the direction of polarization of the exciting light. The fluorescent intensity was found to be zero at zero magnetic field and to increase with increasing field.

Hanle suggested the following classical interpretation of the effect. The exciting light forces elastically bound atomic electrons to oscillate along the direction of polarization $\vec{e}_o$. At zero magnetic field the oscillations are damped and gradually decay because of radiation losses, but the direction of the oscillations is conserved. Because the intensity of radiation emitted by an electric dipole is zero along the axis of the dipole, no fluorescence is observed in the experimental arrangement depicted in Fig. 1. However, in a finite magnetic field, the axis of the dipole oscillations precesses about the direction of the magnetic field, while being simultaneously damped. Thus the

8

Figure 1. The geometrical arrangement used in the original Hanle experiment. $\vec{e}_o$ and $\vec{e}$ are the electric vectors of the incident and emitted radiation, respectively.

Z ($\vec{H}$)

Observation

$\vec{e}$

y

$\vec{e}_0$

x

Excitation

O
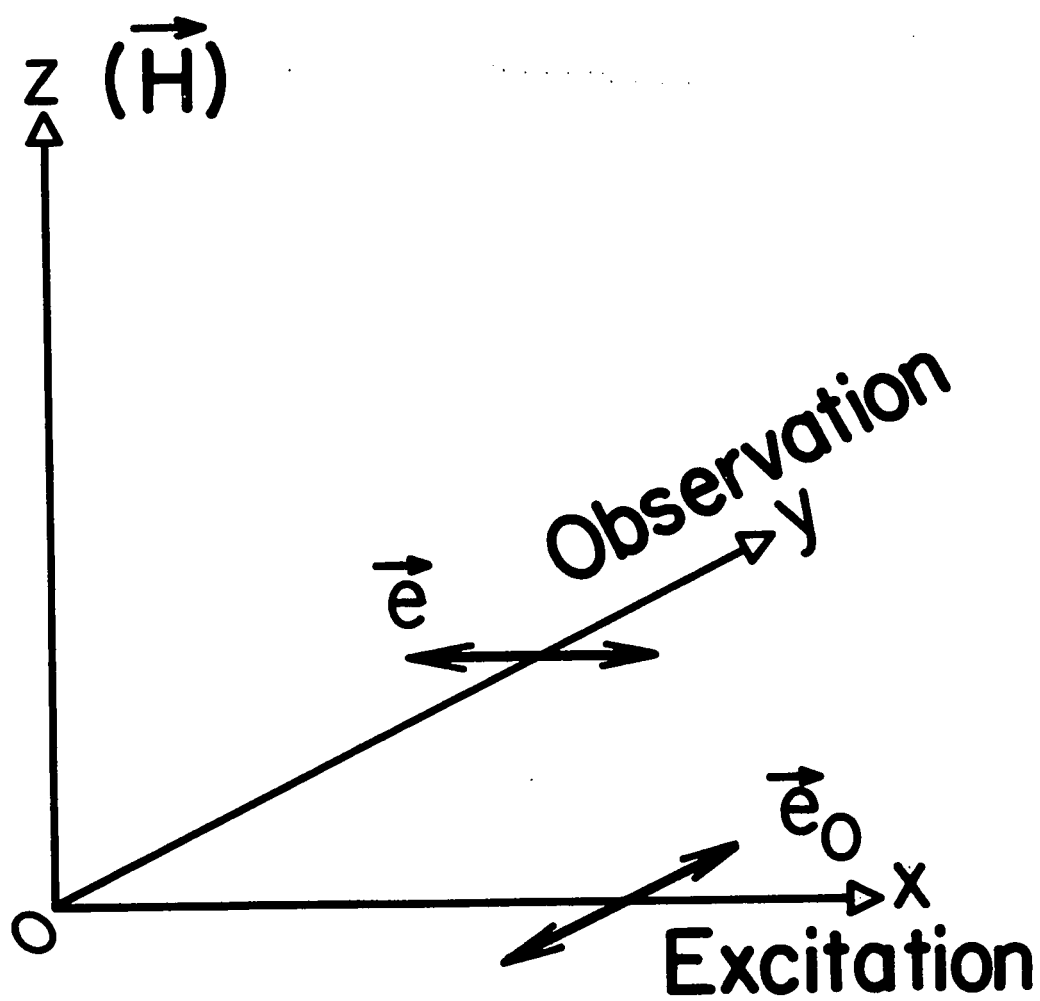
acceleration of the oscillating electron assumes a component
perpendicular to the direction of observation so that some
radiation reaches the detector.

The first quantum-mechanical treatment of the Hanle
effect was developed by Breit (1933) who showed that, if
atoms are excited by light of polarization $\vec{e}_o$, and the
detected fluorescence has polarization $\vec{e}$, then the intensity
$I(\vec{e}_o, \vec{e})$ of the detected radiation is:

$$(2) \qquad I(\vec{e}_o, \vec{e}) =$$

$$CN \sum_{\substack{\mu,\mu' \\ m,m'}} \frac{\langle \mu' | (\vec{p} \cdot \vec{e})^+ | m' \rangle \langle m' | (\vec{p} \cdot \vec{e}_o) | \mu \rangle \langle \mu | (\vec{p} \cdot \vec{e}_o)^+ | m \rangle \langle m | \vec{p} \cdot \vec{e} | \mu' \rangle}{\Gamma_{mm'} + \frac{i}{\hbar} E_{mm'}}$$

where C is an arbitrary constant which depends on the
oscillator strength of the optical transition as well as on
the spectral profile and intensity of the exciting light, N
is the density of atoms in the ground state, $\vec{p}$ is the electric
dipole moment operator and $E_{mm'}$ is the energy difference
between the excited state sublevels m and m'. $\Gamma_{mm'} = 1/2$
$(\Gamma_m + \Gamma_{m'})$, where Γ_m and $\Gamma_{m'}$ are the widths of sublevels
m and m' in the excited state, respectively. The summation
includes all the ground state sublevels μ and μ' and all the
sublevels m and m' of the excited state.

Although the Hanle effect was originally observed
in resonance fluorescence, it may also be produced in
sensitized fluorescence of alkali atoms. Excited and oriented

$^2P_{1/2}$ atoms are produced by irradiating alkali vapour with D_1 (σ^+) light (σ^+ denotes right-handed circular polarization). Sensitizing collisions occurring during the lifetime of the $^2P_{1/2}$ state, cause a transfer of polarization (and of coherence) to the $^2P_{3/2}$ state because, as the result of collisions, the Zeeman substates with negative m_J values are populated preferentially. The relative transition probabilities which have been calculated by Elbel and Naumann (1967), are indicated in Fig. 2 which is applicable in the absence of a magnetic field so that the axis of the incident light beam may be regarded as the axis of quantization. The $^2P_{3/2}$ state populated in this manner, decays with the emission of D_2 (σ^-) light. This may be verified by inspection of the various transition probabilities indicated in Fig. 1, bearing in mind that the circular polarization $I(D_2\sigma^+) - I(D_2\sigma^-)$ of the fluorescence emitted from the $^2P_{3/2}$ state is proportional to the polarization of the state itself. The polarization is represented by $\sum_{m_J} m_J N_{m_J} / \sum_{m_J} N_{m_J}$, where N_{m_J} is the density of atoms in the $|Jm_J\rangle$ state. Thus the transfer of polarization may be studied by monitoring the circular polarization of the D_2 sensitized fluorescence emitted in the backward direction from a sample of alkali vapour excited with $D_1 \sigma^+$ light. The transfer of excitation takes place between polarized atoms precessing in a magnetic field which is perpendicular to the directions of both exciting and fluorescent light beams. The resulting Hanle effect in sensitized fluorescence differs considerably from

Figure 2. The energy levels and transitions involved in the collisional transfer of coherence. Only the transitions from and to the $^2S_{1/2}$ sublevels are radiative in character. The relative transition probabilities are indicated by the thickness of the arrows.
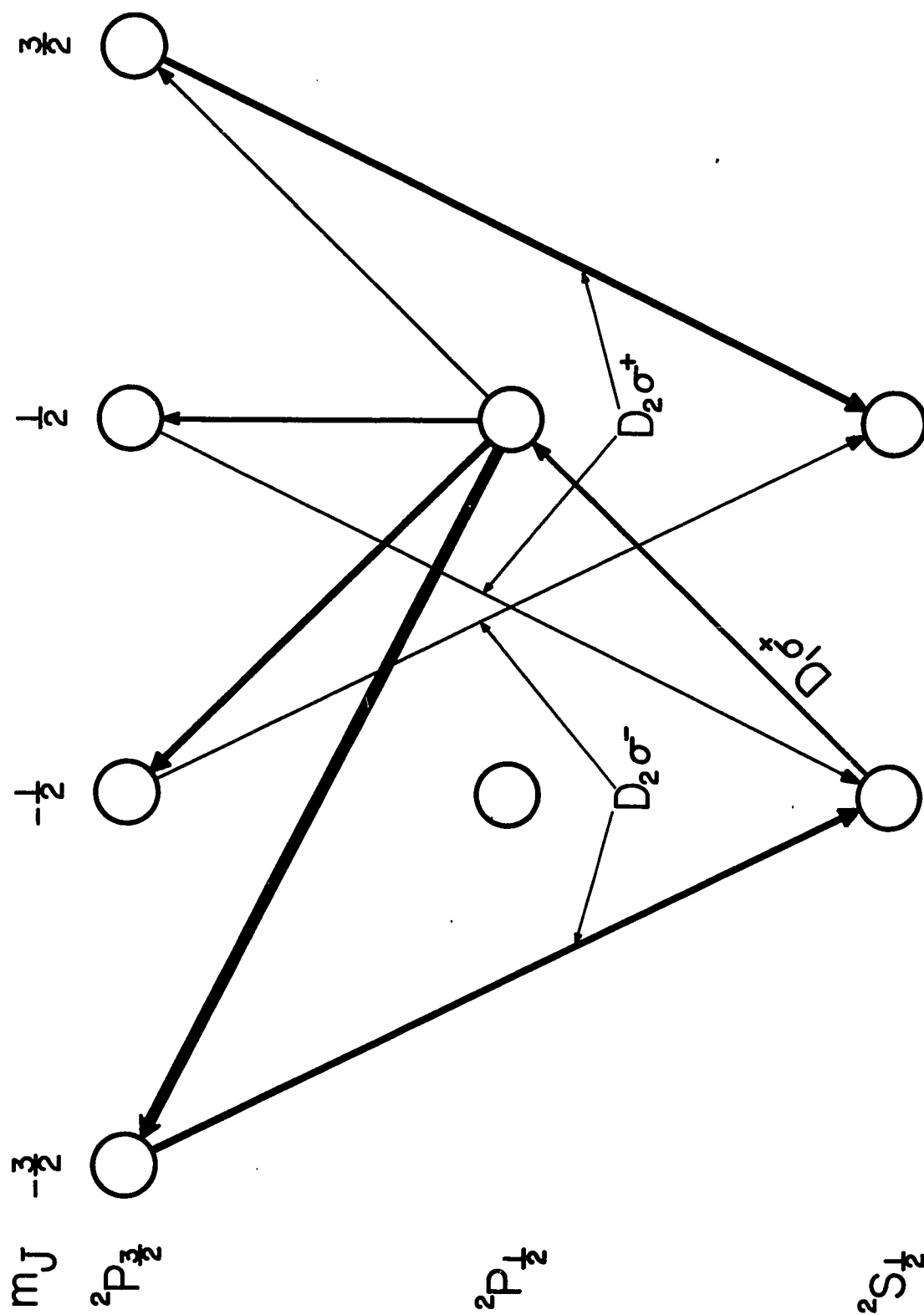
Hanle effect in resonance fluorescence. The rates of precession of the polarization vectors in the $^2P_{1/2}$ and $^2P_{3/2}$ states are different because the respective g_J factors are not equal to one another, and therefore the polarization in the $^2P_{1/2}$ state is not expected to be in phase with the polarization in the $^2P_{3/2}$ state. If several precessions take place during the lifetime of the states, there is no build-up of polarization in the $^2P_{3/2}$ state. This should be observed in strong magnetic fields. However, if the angle swept out during the atomic lifetime is small, the difference in the precession rates will not prevent the establishment of measurable polarization in the $^2P_{3/2}$ state. It should be expected, however, that the "wings" of the Hanle signal in sensitized fluorescence should rapidly decrease in amplitude. On the other hand, the Hanle curves in resonance fluorescence would be expected to decrease in amplitude much more slowly and approach zero asymptotically, since the polarization of resonance fluorescence is affected only by the precession of the axis of electron oscillations and their damping, in accordance with the classical model proposed by Hanle.

The Hanle effect in resonance fluorescence and in sensitized fluorescence may be interpreted on the basis of a model developed by Elbel, Niewitecka and Krause (1970), which describes the precession of the vector polarization about the direction of the magnetic field, taking into account radiation damping and, in the case of sensitized

fluorescence, the transfer of polarization between two atomic states. The description which follows is relevant to the particular arrangement which was employed in this study and which is shown in Fig. 3. A beam of $D_1(\sigma^+)$ light directed along the x-axis excites the alkali atoms in the fluorescence cell which is located at the origin of the coordinate system and in a magnetic field pointing in the direction Oz. The emitted fluorescence is observed at an angle $\alpha < 45^\circ$ to the exciting beam.

1. Hanle Effect in Resonance Fluorescence

The light beam may be described as a series of very short light pulses separated from each other by very small time intervals. The instant at which the light pulse enters the cell is chosen as the origin of the time scale.

The polarization $\vec{p}$ of atoms in the $^2P_{1/2}$ state, established at time t = 0, can be expressed as:

$$(3) \qquad \vec{p}\,(t = 0) = p\,\vec{u}_x \quad ,$$

where $\vec{u}_x$ is a unit vector pointing along the x-axis. As the vector polarization precesses about the direction of the magnetic field, it spontaneously decays with lifetime τ and it is also being destroyed by depolarizing collisions. These two effects cause camping of the vector precession. The total damping rate τ' is given by:

$$(4) \qquad 1/\tau' = 1/\tau + 1/\tau_c \quad ,$$

Figure 3. The arrangement of the exciting and fluorescent light beams with respect to the coordinate axes. The magnetic field is directed along the positive z axis and the fluorescent beam is in the x-y plane.
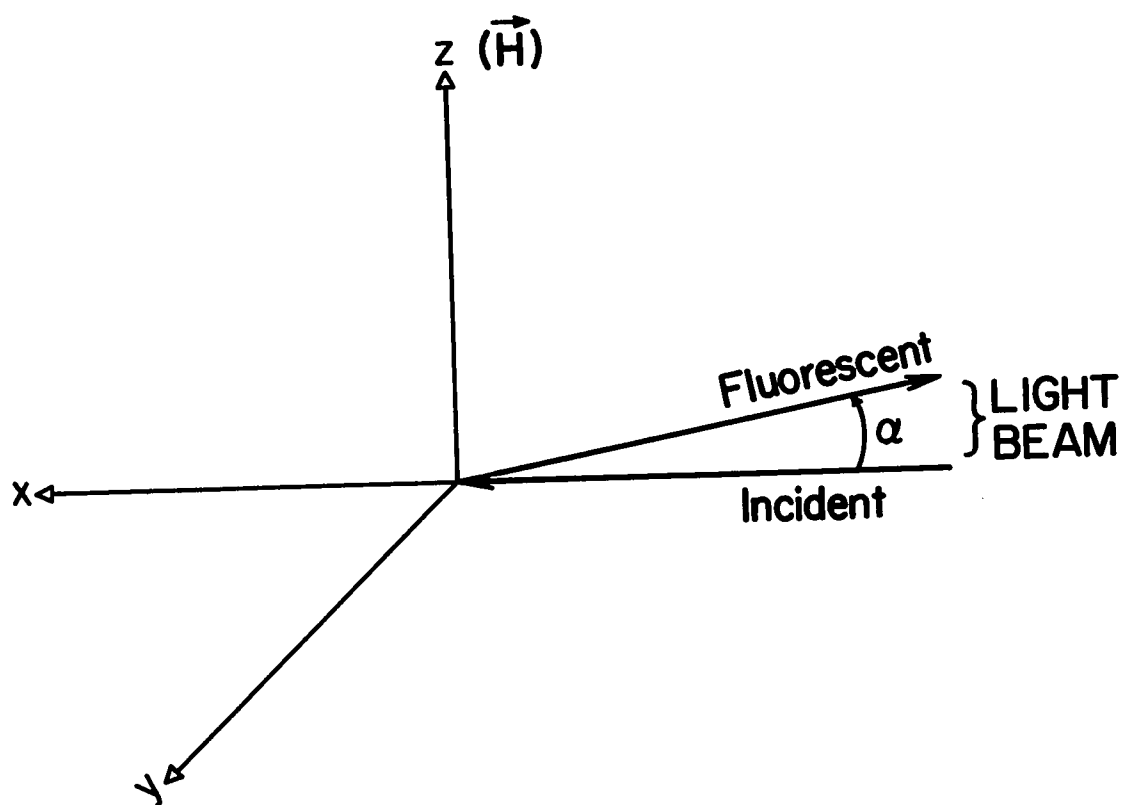
where τ_c is the time between two consecutive collisions. The equation of motion of the vector polarization $\vec{p}$ has the form:

(5)
$$d\vec{p}/dt = \vec{\omega} \times \vec{p} - \frac{\vec{p}}{\tau'} \quad ,$$

where

(6)
$$\vec{\omega} = -\frac{1}{\hbar} g_{1/2} \mu_B \vec{H}$$

ω is the precession frequency in a magnetic field H, $\hbar = h/2\pi$, where $h = 6.6253 \times 10^{-27}$ erg s is the Planck constant, $\mu_B = 9.271 \times 10^{-21}$ erg/gauss is the Bohr magneton and g_J is the Landé factor for the P_J state, defined as follows:

(7)
$$g_J = 1 + \frac{J(J+1) + S(S+1) - L(L+1)}{2J(J+1)}$$

($g_J = 2/3$ for the $^2P_{1/2}$ state and $g_J = 4/3$ for the $^2P_{3/2}$ state). The vector equation (5) may be resolved into three coupled equations describing the x, y and z components of $\vec{p}$.

(8a)
$$dp_x/dt = \omega_y p_z - \omega_z p_y - p_x/\tau'$$

(8b)
$$dp_y/dt = \omega_z p_x - \omega_x p_z - p_y/\tau'$$

(8c)
$$dp_z/dt = \omega_x p_y - \omega_y p_x - p_z/\tau'$$

Because $\omega_x = \omega_y = 0$, eqs. (8a,b,c) simplify to

(9a)
$$dp_x/dt = -\omega p_y - p_x/\tau'$$

(9b) $\qquad dp_y/dt = \omega p_x - p_y/\tau'$

(9c) $\qquad dp_z/dt = - p_z/\tau'$

where $\omega = |\vec{\omega}| = \omega_z$.

Equations (9a,b,c) have solutions of the form

(10a) $\qquad p_x(t) = e^{-t/\tau'} \cos \omega t$

(10b) $\qquad p_y(t) = e^{-t/\tau'} \sin \omega t$

(10c) $\qquad p_z(t) = e^{-t/\tau'}$

$p_z \to 0$ as $t \to \infty$, and is negligible. Using Eqs. (10a) and (10b) the polarization of resonance fluorescence observed at an angle α to the incident beam may be expressed as follows:

(11) $\qquad p(\alpha, t) = p_x(t) \cos \alpha + p_y(t) \sin \alpha$

$\qquad = e^{-t/\tau'} \cos \omega t \cos \alpha + e^{-t/\tau'} \sin \omega t \sin \alpha$

The observed difference between the intensities of clockwise and anticlockwise components of the circularly polarized fluorescent light emitted at an angle α by alkali vapour which had been excited with a light pulse at time $t = 0$ is directly proportional to $p(\alpha, t)$. However, fluorescence is also observed, which is produced at time t' by exciting pulses arriving earlier than at t. Thus the expression for $p(\alpha, t-t')$ must be integrated over the values of $(t-t')$ from $-\infty$ to 0.

$$(12) \quad I_{\sigma^+}^{(1/2)} - I_{\sigma^-}^{(1/2)} \propto \int_{(t-t')=-\infty}^{0} p(\alpha, t-t') \, d(t-t')$$

$$\propto \frac{\cos \alpha + \omega\tau' \sin \alpha}{1/\tau'^2 + \omega^2}$$

Equation (12) can be fitted directly to the experimental Hanle curves in resonance fluorescence using the factor ($\omega\tau'$) as an adjustable parameter.

2. Hanle Effect in Sensitized Fluorescence

The polarization induced in the $^2P_{1/2}$ state is partly destroyed as the result of depolarizing collisions with buffer gas atoms or molecules. Many of the collisions cause transfer of excitation energy to the $^2P_{3/2}$ state, which may be accompanied by the simultaneous transfer of polarization (coherence) from the $^2P_{1/2}$ state. The transferred polarization vector precesses about the magnetic field with a frequency $\vec{\Omega}$ given by:

$$(13) \quad \vec{\Omega} = -\frac{1}{\hbar} g_{3/2} \mu_B \vec{H} .$$

The polarization in the $^2P_{3/2}$ state decays with a time constant τ'' which, in general, differs from τ' since the rate of collisional depolarization in the $^2P_{3/2}$ state may be different from that in the $^2P_{1/2}$ state. When the decay of polarization is due mainly to spontaneous decay rather than to collisional depolarization, it may be assumed that the time constants τ' and τ'' both approach a common value τ. The equation of motion of the polarization vector $\vec{P}$ in the

$^2P_{3/2}$ state has the form

$$(14) \qquad d\vec{P}/dt = \vec{\Omega} \times \vec{P} - \frac{\vec{P}}{\tau''} + A\vec{p} \quad .$$

The last term in Eq. (14) represents an inhomogeneity of this differential equation and couples it to Eq. (5), as it represents a gain of polarization from the $^2P_{1/2}$ state through sensitizing collisions. As may be seen in Table I, at buffer gas pressures of approximately 1 torr, the time τ_c between two consecutive collisions is shorter than the natural lifetime τ of the ^2P states in sodium and potassium. Thus collisional back-transfer of polarization $\vec{P}$ to the $^2P_{1/2}$ state is considered negligible since it would require a second collision during the natural lifetime of the $^2P_{3/2}$ state. Equation (14) may be treated similarly as Eq. (5) and may be resolved into three separate equations representing components of the vector $\vec{P}$. Since in the present case $\Omega_x = \Omega_y = 0$, only the following two equations need be considered.

$$(15a) \qquad dP_x/dt = -\Omega P_y - P_x/\tau'' + Ap_x$$

$$(15b) \qquad dP_y/dt = +\Omega P_x - P_y/\tau'' + Ap_y$$

where $\Omega = |\vec{\Omega}| = \Omega_z$.

Assuming $\tau' = \tau'' = \tau$ and substituting for p_x and p_y from Eqs. (10a) and (10b) respectively, the solutions of Eqs. (15a) and (15b) may be written as,

$$(16a) \qquad P_x = Ap \frac{\sin \Omega t - \sin \omega t}{\Omega - \omega} e^{-t/\tau}$$

(16b)
$$P_y = Ap \frac{\cos \Omega t - \cos \omega t}{\Omega - \omega} e^{-t/\tau}$$

where $p = \sqrt{p_x^2 + p_y^2} = e^{-t/\tau}$. The projection of $\vec{P}$ on the fluorescent light beam axis is given by:

(17)
$$P(\alpha,t) = P_x(t) \cos \alpha + P_y(t) \sin \alpha$$

The integration of Eq. (17) over time, similarly as was done with Eq. (12), yields the following expression for the polarization of the sensitized fluorescence.

(18)
$$I_{\sigma^+}^{(3/2)} - I_{\sigma^-}^{(3/2)} \propto \frac{\cos \alpha}{\Omega - \omega} \left[\frac{\Omega}{\Omega^2 + 1/\tau^2} - \frac{\omega}{\omega^2 + 1/\tau^2} \right]$$
$$+ \frac{\sin \alpha}{\tau} \frac{(\Omega + \omega)}{(\Omega^2 + 1/\tau^2)(\omega^2 + 1/\tau^2)}$$

Equation (18) can also be fitted to an experimental Hanle signal obtained in sensitized fluorescence. The factor $\omega\tau$ is obtained from the fit of Eq. (12) to the Hanle signal in resonance fluorescence at a given buffer gas pressure. The only remaining adjustable parameter is the ratio ω/Ω.

3. The Cross Section for $^2P_{1/2} \rightarrow {}^2P_{3/2}$ Coherence Transfer

The density matrix formalism in its irreducible tensor representation (Fano, 1957; Happer, 1972) may be employed to derive an expression for the coherence transfer cross section. The density matrix may be represented as follows:

(19)
$$\rho^{Jm_J} = \sum_{xq} \rho_x^{(q)} [T_x^{(q)}]^{Jm_J} \quad ,$$

where $T_x^{(q)}$ is an irreducible tensor operator of rank x

($0 \leq x \leq 2J$), q is a component of the 2x-pole moment and

$\rho_x^{(q)}$ is the density of the q-th component of the 2x-pole

moment of the ensemble of atoms in the $|J\rangle$ state.

In applying Eq. (19) to represent the density matrix

of an excited state such as $^2P_{1/2}$ or $^2P_{3/2}$ it is assumed

that all off-diagonal elements may be neglected. This

assumption is valid in the absence of a magnetic field when

the collisions are isotropic (q = 0), and when nuclear spin

is neglected. Under isotropic conditions, when each

multipole component of the polarization is decoupled from

the other multipole transition components, the density

matrix for the $^2P_{3/2}$ state has the explicit form:

$$(20) \qquad \rho^{(3/2,m_J)} = [\rho_0 T_0^{(3/2,m_J)} + \rho_1 T_1^{(3/2,m_J)}$$

$$+ \rho_2 T_2^{(3/2,m_J)} + \rho_3 T_3^{(3/2,m_J)}]$$

where ρ_0 is the measure of the total population of atoms

in the $|3/2,m_J\rangle$ state, ρ_1 corresponds to the overall

density of magnetic dipoles associated with atoms excited to

the $|3/2,m_J\rangle$ state, and ρ_2 and ρ_3 represent quadrupole

and octupole magnetic moment densities in the $|3/2,m_J\rangle$

state, respectively. According to D'yakonov and Perel'

(1965), neither quadrupole nor octupole magnetic moments

can be produced in the $^2P_{3/2}$ state as the result of

collisional transfer from oriented $^2P_{1/2}$ atoms. Consequently,

Eq. (20) has the form:

$$(21) \qquad \rho^{3/2,m_J} = \rho_0 T_0^{3/2,m_J} + \rho_1 T_1^{3/2,m_J} .$$

Because only the diagonal elements of the density matrix need be considered, the density matrix may be replaced by the population vector $\vec{N}^J$:

$$(22) \qquad \vec{N}^{(3/2)} = \begin{pmatrix} N_{3/2}^{(3/2)} \\ N_{1/2}^{(3/2)} \\ N_{-1/2}^{(3/2)} \\ N_{-3/2}^{(3/2)} \end{pmatrix} = N_0^{(3/2)} T_0^{(3/2)} + N_1^{(3/2)} T_1^{(3/2)}$$

where

$$(23) \qquad T_0^{(3/2)} = \frac{1}{2} \begin{pmatrix} 1 \\ 1 \\ 1 \\ 1 \end{pmatrix} \quad ; \quad T_1^{(3/2)} = \frac{1}{2\sqrt{5}} \begin{pmatrix} 3 \\ 1 \\ -1 \\ -3 \end{pmatrix}$$

$N_0^{(J)}$ is the total density of atoms in the $|J\rangle$ state and $N_1^{(J)}$ is the total density of the magnetic dipole moment in the $|J\rangle$ state. Since $T_0^{(3/2)}$ and $T_1^{(3/2)}$ are orthonormal, the scalar product of Eq. (22) and $T_1^{(3/2)}$ will have the form:

$$(24) \qquad N_1^{(3/2)} = T_1^{(3/2)} \cdot N^{(3/2)} = \frac{1}{2\sqrt{5}}$$
$$\times (3N_{3/2}^{(3/2)} + N_{1/2}^{(3/2)} - N_{-1/2}^{(3/2)} - 3N_{-3/2}^{(3/2)})$$

Equation (24) establishes a direct connection between $N_1^{(3/2)}$ and the polarization of the observed D_2 fluorescence, since the decay of the $m_J = 1/2, 3/2$ substates gives rise to the σ^+ component of the fluorescence and the decay of the $m_J = -1/2, -3/2$ substates to the σ^- component. Equation (24) may be expressed in terms of the components I_{σ^+} and I_{σ^-} of the observed fluorescence

$$(25) \qquad N_1^{(3/2)} = \frac{1}{2\sqrt{5}} \; \frac{1}{h \cdot v_2 \, A_2} \, (I_{\sigma^+}^{(3/2)} - I_{\sigma^-}^{(3/2)})$$

where $I_{\sigma^+}^{(3/2)}$ and $I_{\sigma^-}^{(3/2)}$ are the relative intensities of circularly polarized components of the D_2 fluorescence emitted in the decay of the $^2P_{3/2}$ state, v_2 is the optical frequency of the D_2 radiation and A_2 is the $P_{3/2} \to S_{1/2}$ transition probability. Thus the polarization of sensitized fluorescence depends only on the net density of the magnetic dipole moment or on the density of orientation in the $P_{3/2}$ state.

A similar argument may be used to express the density of orientation in the $^2P_{1/2}$ state in terms of the polarization of the D_1 fluorescence. Since a $^2P_{1/2}$ atom can possess only a dipole moment, the density matrix may be written as follows:

$$(26) \qquad \rho^{1/2, m_J} = (\rho_0 T_0^{(1/2)} + \rho_1 T_1^{(1/2)}).$$

In the absence of off-diagonal elements,

$$(27) \quad \vec{N}^{(1/2)} = \begin{pmatrix} N_{1/2}^{(1/2)} \\ N_{-1/2}^{(1/2)} \end{pmatrix} = N_o^{(1/2)} T_o^{(1/2)} + N_1^{(1/2)} T_1^{(1/2)} ,$$

where

$$(28) \quad T_o^{(1/2)} = \frac{1}{\sqrt{2}} \begin{pmatrix} 1 \\ 1 \end{pmatrix} ; \quad T_1^{(1/2)} = \frac{1}{\sqrt{2}} \begin{pmatrix} 1 \\ -1 \end{pmatrix} .$$

Using an argument analogous to that employed in deriving Eqs. (24) and (25),

$$(29) \quad N_1^{(1/2)} = \frac{1}{2\sqrt{2}} (N_{1/2}^{(1/2)} - N_{-1/2}^{(1/2)}) = \frac{1}{2\sqrt{2}} \frac{1}{h \, \upsilon_1 A_1} (I_{\sigma^+}^{(1/2)}$$

$$- I_{\sigma^-}^{(1/2)}) ,$$

where υ_1 is the optical frequency of the D_1 radiation, A_1 is the $^2P_{1/2} - {}^2S_{1/2}$ transition probability and all other quantities are defined as in Eqs. (24) and (25). It should be borne in mind that the above considerations do not take into account nuclear spin. The influence of nuclear spin would be represented by the appearance of two additional expressions representing the off-diagonal terms of the dipole components of the density matrices: $\rho_{1\pm1}^{(1/2)}$ and $\rho_{1\pm1}^{(3/2)}$. However, because the fluorescence is being observed in an approximately backward direction, the contributions arising from the off-diagonal terms (representing alignment) would contribute very little to the signal. (The contribution due to the off-diagonal terms is proportional to $\sin^2 21°$.)

The rate of change of the population of the oriented

$^2P_{3/2}$ atoms may be described by the following equation.

(30) $\qquad dN_1^{(3/2)}/dt = -1/\tau \; N_1^{(3/2)} - Z_D N_1^{(3/2)} + Z_C N_1^{(1/2)}$

where Z_D and Z_C are the frequencies of disorienting and of "coherence transfer" collisions per oriented ^2P atom, respectively, and τ is the mean lifetime of the $^2P_{1/2}$ or $^2P_{3/2}$ state in sodium or potassium (see Table I).

Assuming stationary conditions, $\dot{N}_1^{(3/2)} = 0$ and Eq. (30) reduces to:

(31) $\qquad Z_C = \left[N_1^{(3/2)}/N_1^{(1/2)} \right] (1/\tau + Z_D) \quad .$

The ratio $N_1^{(3/2)}/N_1^{(1/2)}$ can be expressed in terms of experimentally measured polarization, using Eqs. (25) and (29):

(32) $\qquad N_1^{(3/2)}/N_1^{(1/2)} = \sqrt{2/5} \left[\dfrac{I_{\sigma^+}^{(3/2)} - I_{\sigma^-}^{(3/2)}}{I_{\sigma^+}^{(1/2)} - I_{\sigma^-}^{(1/2)}} \right] \dfrac{\upsilon_1}{\upsilon_2}$

It may be assumed to a good approximation that $\upsilon_1/\upsilon_2 = 1$ for sodium and for potassium. The transition probabilities A_1 and A_2 are equal in both sodium and potassium so that $A_1 = A_2$. The net polarization of the sensitized fluorescence $(I_{\sigma^+}^{(3/2)} - I_{\sigma^-}^{(3/2)})$ is proportional to the orientation of the $^2P_{3/2}$ atoms, induced in collisional coherence transfer from the $^2P_{1/2}$ state in which the atoms had been oriented by excitation with $D_1(\sigma^+)$ light. $(I_{\sigma^+}^{(1/2)} - I_{\sigma^-}^{(1/2)})$ represents the net polarization of the resonance fluorescence and is proportional to the orientation of the $^2P_{1/2}$ atoms

(Elbel, Niewitecka and Krause, 1970).

The total disorientation cross sections Q_D and coherence transfer cross sections Q_C are defined by analogy with the gas kinetic collision cross section,

$$(33) \qquad Z_D = N \ v_r \ Q_D \ ,$$

$$(34) \qquad Z_C = N \ v_r \ Q_C \ .$$

Eqs. (31), (32), (33) and (34) together yield the final expression for Q_C:

$$(35) \qquad Q_C = \sqrt{2/5} \left[\frac{I_{\sigma^+}^{(3/2)} - I_{\sigma^-}^{(3/2)}}{I_{\sigma^+}^{(1/2)} - I_{\sigma^-}^{(1/2)}} \right] \left(Q_D + \frac{1}{\tau \ N \ v_r} \right)$$

Eq. (35) provides the connection between the cross sections for coherence transfer and measured fluorescent intensities. It contains also disorientation cross sections whose effect on the coherence cross section will be discussed in a subsequent chapter.

The coherence transfer cross section is related only to the fraction of polarization transferred from the $^2P_{1/2}$ state to the $^2P_{3/2}$ state which remains unaffected by the influence of nuclear spin. However, presence of a nuclear spin will cause a certain amount of "spontaneous disorientation" in the $^2P_{1/2}$ state, arising from I-J precession whose period in this state is comparable with the ^2P lifetime both for sodium and for potassium, as it may be noticed from the data in Table I. The "spontaneous disorientation" in the $^2P_{3/2}$ state is negligible because the I-J precession in

this state has a period about two and three times longer for sodium and potassium, respectively, than the ^2P lifetime.

III. EXPERIMENTAL

1. Description of the Apparatus

The arrangement of the apparatus is shown in Fig. 4. An Osram lamp which was used in the investigation of coherence transfer in sodium, or an r.f. electrodeless discharge in the case of potassium, provided the source of alkali resonance radiation. The light emitted by the lamp was rendered parallel, was resolved by interference filters, circularly polarized, and was made incident on alkali vapour mixed with a buffer gas and contained in a fluorescent cell. The latter was mounted in a constant-temperature oven and located at the centre of a set of Helmholtz coils. The resulting fluorescence was analysed with respect to its wavelength and circular polarization, and was focused on the photocathode of a photomultiplier whose output was applied to a phase-sensitive amplifier or to a picoammeter and was registered with a strip-chart recorder.

The exciting light beam was first passed through a pair of Spectrolab interference filters which transmitted only the D_1 component of the resonance doublet. The spectral purity of the D_1 component was of the order of one part in 10^4. The D_1 radiation was then circularly polarized by a combination of a linear polarizer (Polaroid type HN7)

28

Figure 4. The arrangement of the apparatus. A, spectral lamp; C, fluorescence cell in oven; D_1, D_2, interference filters; L, lenses; M, picoammeter; P, linear polarizers; PM, photomultiplier tube; R, recorder; S, slit; $\lambda'/4$, $\lambda''/4$, quarter-wave plates.
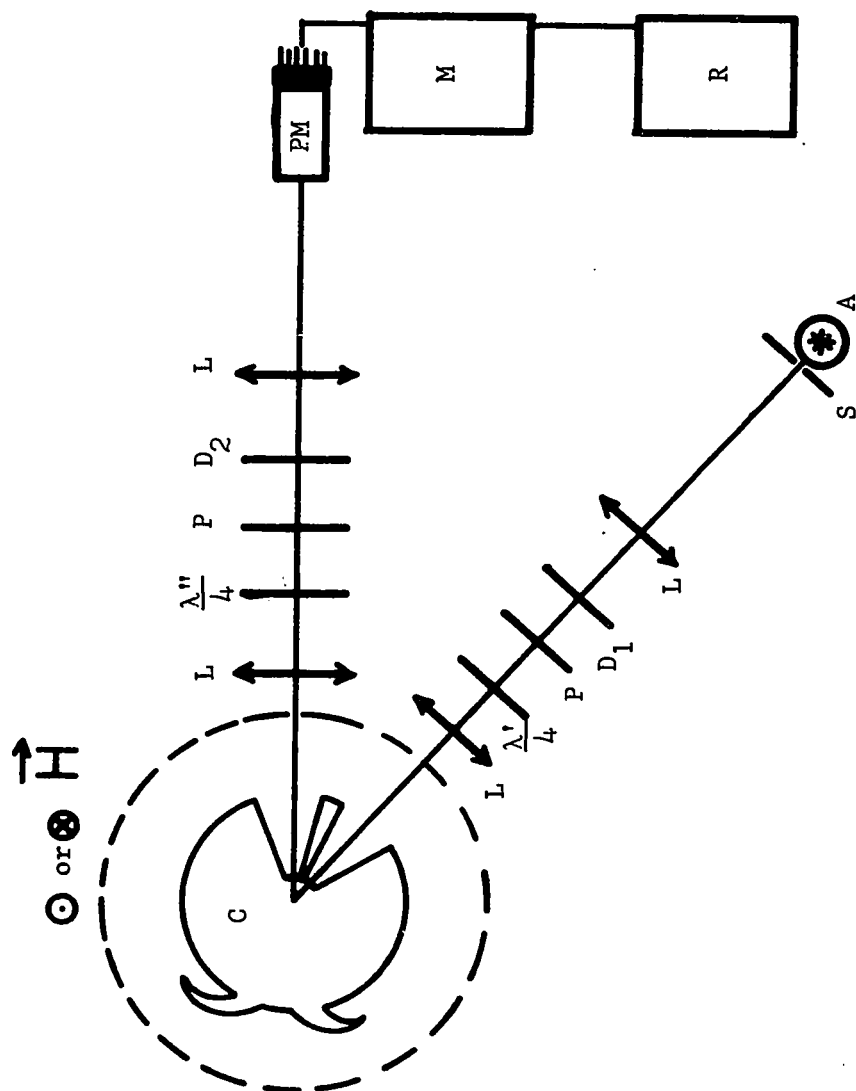
and a properly oriented quarter-wave plate selected for the particular wavelength. The resulting $D_1\sigma^+$ light was brought to a focus at the centre of the spherical fluorescence cell fitted with two plane windows.

Two fluorescent cells which are shown in Figs. (5a) and (5b), were used at various times: in one the window axes were inclined at an angle of $35°$ to each other and in the other at $42°$. The cell shown in Fig. (5b) afforded a much shorter exciting and fluorescent light path than that shown in Fig. (5a). The optical path in the "a" cell was 13 cm as compared to about 1 cm in the "b" type which was used in all of the experiments except for those with Na-He mixtures (Elbel, Niewitecka and Krause, 1970). The fluorescence cell was painted with aquadag to reduce stray light and was mounted in a double-walled oven. Heating elements mounted on the walls of the inner box were wound non-inductively of Chromel #24 wire. The temperature of the oven was maintained constant to within $\pm 1°C$ over long periods of time. The cell was equipped with a side-arm which contained the liquid alkali metal and which was contained in a separate oven whose temperature was kept constant within $\pm 0.1°C$ by means of oil circulating from a Haake ultrathermostat. The temperature of the main oven was kept at approximately $20°C$ higher than the temperature of the side-arm in order to prevent condensation of the metal on the cell windows. The temperatures in both ovens were monitored by six chromel-alumel thermocouples attached to

Figure 5a. Top view and a side view of a fluorescence cell with an angle of 35°

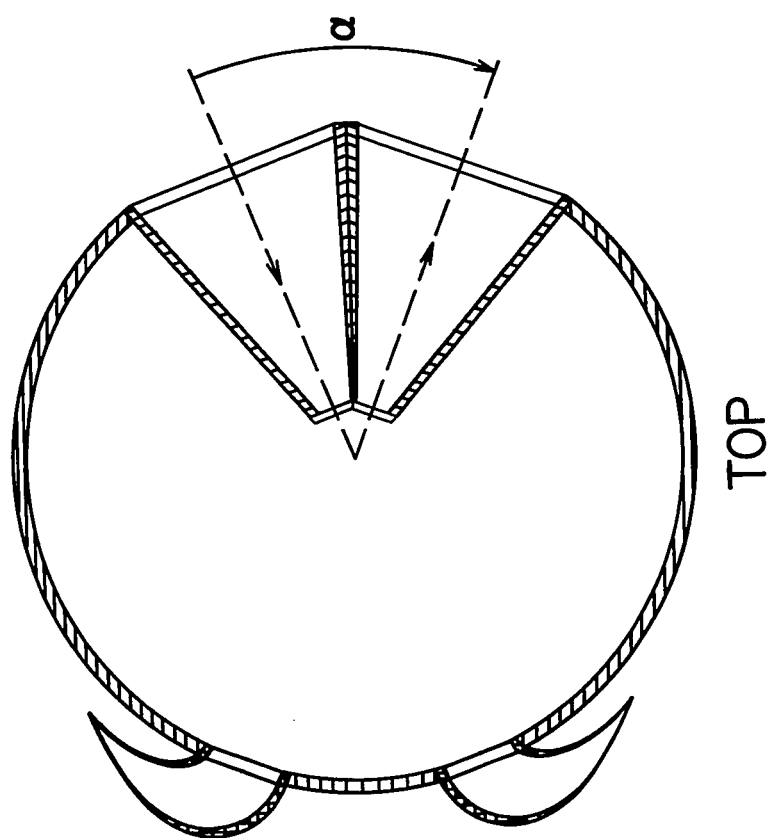between the axes of excitation and observation.

SIDE

OIL

α

TOP
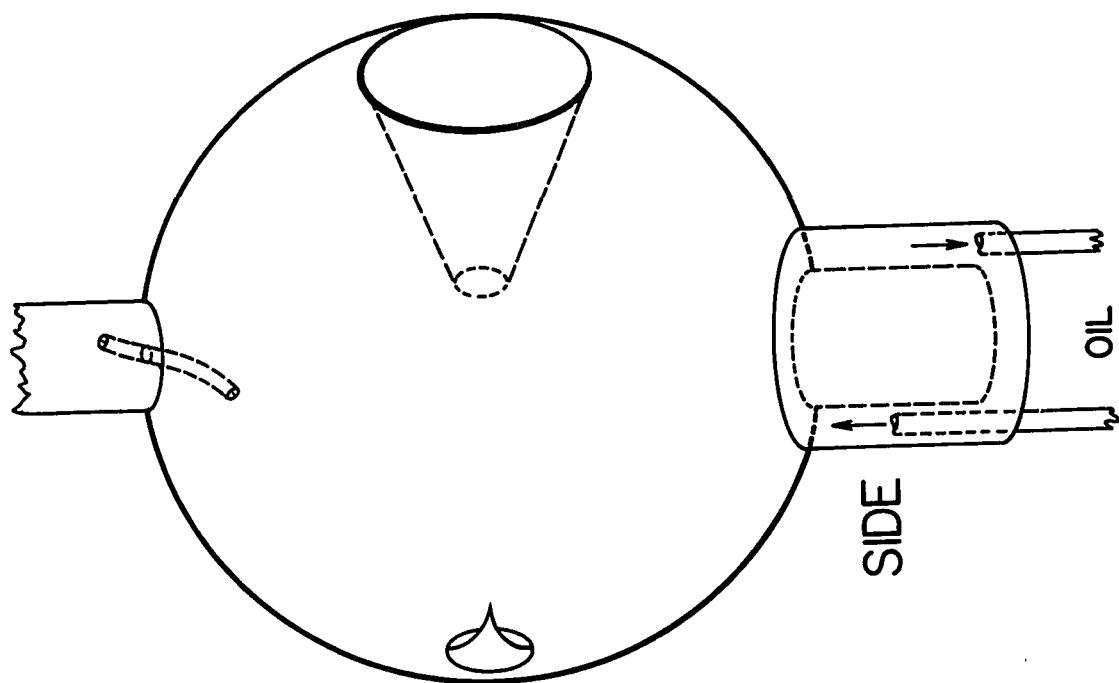
Figure 5b. Top view and a side view of a fluorescence cell with an angle of 42° between the axes of excitation and observation.

SIDE

TOP

α
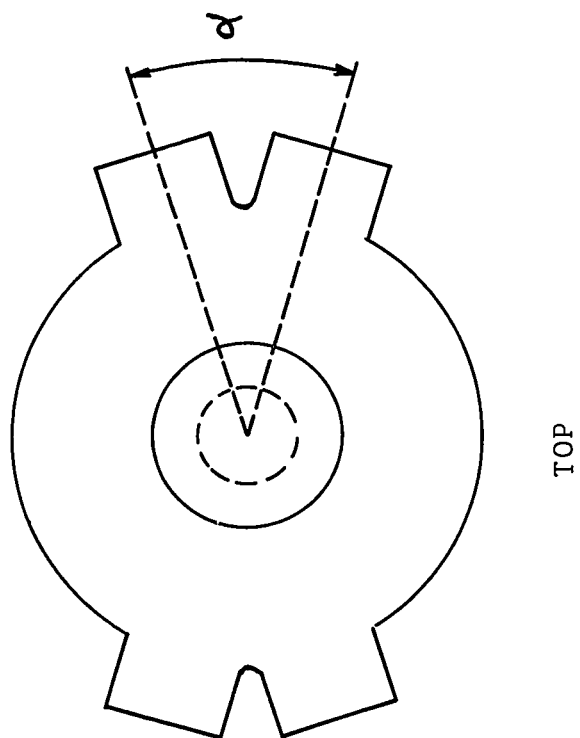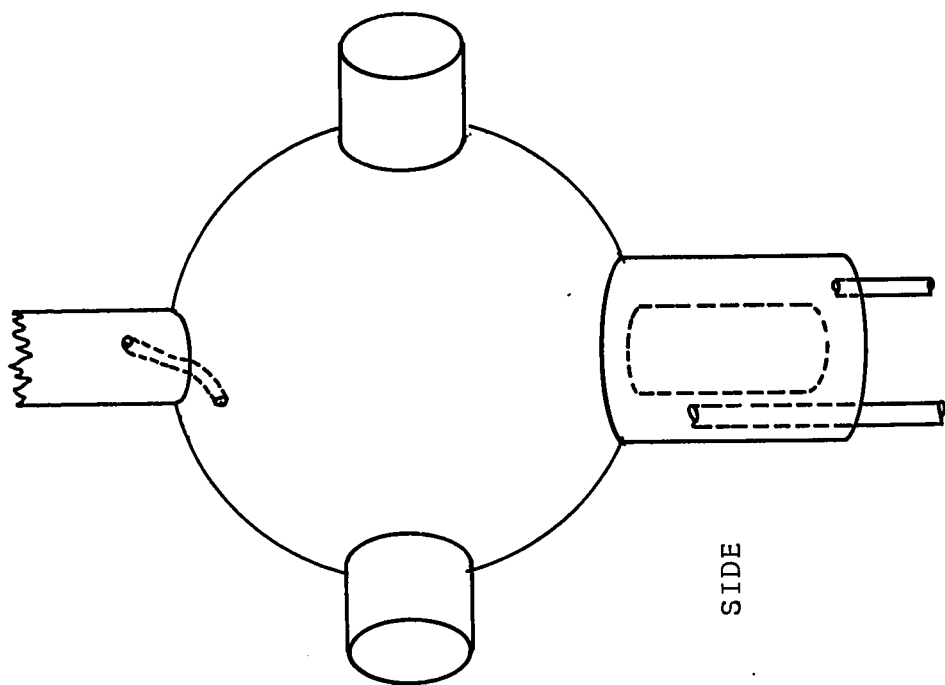
various points on the cell and side-arm, and connected to a Leeds and Northrup 8686 millivolt potentiometer.

The fluorescence cell was connected to a vacuum and gas-filling system by a narrow-bore tube. The cell was evacuated by an Edwards EO2 diffusion pump equipped with a cold trap containing a copper foil getter, and backed by an Edward ES35 rotary pump. The lowest pressure obtained consistently was about 5×10^{-8} torr and was measured with a Consolidated Vacuum GIC-300 ionization gauge equipped with a GIC-017 gauge head (10^{-4}-10^{-10} torr). The buffer gas pressures ranging from 10^{-3} torr to 10 torr were measured with an accuracy of ± 0.01 torr with a liquid-air trapped C.V.C. McLeod gauge type GM-100A and were corrected for transpiration effects according to the expression:

$$(36) \qquad \frac{P}{P'} = \sqrt{\frac{T}{T'}}$$

where P is the pressure in the cell, P' is the pressure measured by the McLeod gauge at room temperature, T is the absolute temperature in the cell and T' is the room temperature in degrees K. The spectroscopically pure gases used in the experiments were obtained in one-litre pyrex bulbs from the Linde Company. Before being admitted to the cell, the gases were gettered for several days with hot potassium or rubidium vapour.

The cell and oven were located at the centre of a pair of Helmholtz coils which produced a vertical magnetic field perpendicular to the excitation-observation plane.

The coils had an inside diameter of 38 cm and each consisted of 255 turns of Anofol (oxidized aluminum) ribbon 7.2 cm wide and 0.02 cm thick. The set generated a magnetic field of 9.7 G/A. Current to the coils was supplied from a Hewlett-Packard 6269-B DC power supply (rated at 0-40 V and 0-50 A), and was stabilized within $\pm$0.5%. The magnetic field at the centre of the coils was homogeneous to $\pm$0.2% within 5 cm from the axis of the coils. The region of observation in the vapour, located in the centre of the coils had a maximal radius of 2.5 cm using the cell shown in Fig. (5a), and 0.5 cm with the cell shown in Fig. (5b). Thus, the magnetic field in the fluorescing region had a homogeneity better than $\pm$0.1%.

An ITT FW-118 photomultiplier with S-1 spectral response was used for the detection of the potassium fluorescence but sodium fluorescence was detected with a Philips 56TVP tube which had S-20 spectral response, and later with an RCAC31031 photomultiplier. All photomultipliers were cooled with liquid nitrogen and were enclosed in a netic-conetic antimagnetic shield. During the d.c. measurements the output of the photomultiplier was amplified with a Keithley Model 417 picoammeter and was recorded with a Hewlett-Packard 7101B strip-chart recorder. When phase-sensitive detection methods were deemed preferable, a quarter-wave plate in the exciting light beam was rotated with a period of 0.116s, producing an alternating clockwise-anticlockwise circular polarization of the exciting radiation.

A reference light beam was chopped synchronously with the rotating quarter-wave plate and was monitored with a photocell; its signal was applied to the reference input of the lock-in amplifier (PAR HR-8), whose output was recorded on a Moseley strip-chart recorder.

2. Experimental Procedure

The fluorescence cell was thoroughly cleaned before use with potassium dichromate cleaning solution followed by distilled water. The cell was then connected through the side-arm to the vacuum system, evacuated and outgassed. Approximately 1 g of alkali metal was distilled into the side-arm. (Ampoules with 99.95% pure sodium or potassium metal were obtained from the A. D. MacKay Company of New York.) The side-arm was then sealed off, the cell was coated with aquadag and was positioned in the oven. After a final alignment of the optics and cell to eliminate scattered light, the cell was fastened and connected to the vacuum system through the capillary tube.

The temperature of the side-arm was kept at all times sufficiently low to ensure the absence of radiation trapping. For sodium, this amounted to $112^{\circ}C$ which was equivalent to a sodium vapour pressure of 3.8×10^{-7} torr. In the case of potassium, the side-arm temperature was maintained at $61^{\circ}C$ which corresponded to a vapour pressure of 6.8×10^{-7} torr. It has been previously found by Kibble, Copley and Krause (1967) and by Copley and Krause (1969) that at these pressures the effects of radiation trapping in sodium

and potassium vapours are negligible. It has also been
pointed out by Hanle (1927) that resonance fluorescence
becomes depolarized with increasing pressure of metal vapour,
as a result of multiple scattering of the resonance radiation.
It was found experimentally that under the conditions
prevailing in this investigation there was no depolarization
arising from multiple scattering of the fluorescence. In
order to prevent condensation of alkali metal on the cell
windows the temperature of the main oven was kept at $148^{\circ}C$
for sodium and at $100^{\circ}C$ for potassium.

Three separate types of observations were carried
out in the course of this investigation, each requiring a
specific procedure.

(i) <u>Hanle</u> <u>Effect</u> <u>in</u> <u>Resonance</u> <u>Fluorescence</u>

Mixtures of alkali vapour and buffer gases were
irradiated in turn with σ^{+} and σ^{-} circularly polarized D_2
resonance radiation and the intensity as well as circular
polarization of the resulting D_2 resonance fluorescence
was determined for both polarizations of the exciting light.
The difference of intensities $I_{\sigma^{+}}^{(3/2)} - I_{\sigma^{-}}^{(3/2)}$ which, as
indicated by Eq. (12), is directly proportional to the
polarization of resonance fluorescence, was found over a
range of magnetic field extending approximately from $-80G$
to $+80G$.

(ii) <u>Hanle</u> <u>Effect</u> <u>in</u> <u>Sensitized</u> <u>Fluorescence</u>

The alkali vapour-buffer gas mixtures were excited
with $D_1(\sigma^{+})$ and $D_1(\sigma^{-})$ radiation in turn and the intensities

of the $D_2(\sigma^+)$ and $D_2(\sigma^-)$ components of the sensitized fluorescence were recorded for both σ^+ and σ^- polarizations of the exciting radiation. The resulting values $I_{\sigma^+}(3/2) - I_{\sigma^-}(3/2)$ were determined in relation to the magnetic field. These determinations were carried out with sodium-noble gas mixtures in magnetic fields ranging from -80G to 80G, and with potassium-helium and potassium-neon mixtures in fields ranging from -30G to +30G. In each case the magnetic field was varied in approximately 2.5 G steps.

(iii) The Determination of the Polarization Ratio $V = \left[I_{\sigma^+}(3/2) - I_{\sigma^-}(3/2)\right] / \left[I_{\sigma^+}(1/2) - I_{\sigma^-}(1/2)\right]$

The circular polarization of the D_1 and D_2 fluorescent components was determined at zero magnetic field with the alkali vapour-buffer gas mixture being irradiated in turn with $D_1(\sigma^+)$ and $D_1(\sigma^-)$ light. The relative intensities of the $D_1(\sigma^+)$ and $D_1(\sigma^-)$ resonance fluorescence as well as of the $D_2(\sigma^+)$ and $D_2(\sigma^-)$ sensitized fluorescence were determined at each buffer gas pressure and keeping the same excitation conditions throughout. The measurements were carried out in the absence of magnetic field to satisfy the conditions postulated in the derivation of Eq. (35). The polarization ratio V was determined several times at each of 8 different buffer gas pressures below 1.5 torr. The determinations necessitated measurements of relative intensities of all four $D(\sigma)$ components which could only be carried out if the transmissions of all the filters were known. These

transmissions were measured in situ and the results are
listed in Table II. The transmissions of the quarter-wave
plates and HN-7 polarizers were found to be 80% and 53%,
respectively.

The feasibility of determining the polarization of
the sensitized fluorescence in potassium depended critically
on the conditions of the experiment. The side-arm tempera-
ture had to be kept at 61^{0}C to ensure the required low
potassium vapour pressure of 6.5×10^{-7} torr which in turn
limited the intensity of the resonance fluorescence to the
extent such that it resulted in a photomultiplier signal of
the order of 10^{-8} A. It was also found that the polarization
of sensitized fluorescence in potassium-noble gas mixtures
decreased dramatically with the pressure of the buffer gas.
For example, the polarization was completely destroyed at
helium pressures greater than 1.7 torr. Thus it was not
possible to increase the buffer gas pressure in order to
increase the overall intensity of sensitized fluorescence
which increases substantially with buffer gas pressure in
the region of 1 torr (Chapman, 1965), where the ratio of
sensitized-to-resonant fluorescent intensities increases
from about 8×10^{-2} at 0.2 torr He to 0.4 at 1 torr He.
The situation is even less favourable with other noble gases
and, as the result, the photomultiplier signal resulting
from the sensitized fluorescence was of the order of 10^{-10} A
at buffer gas pressures of about 1 torr.

TABLE II

Transmissions of the Interference Filters

for D_1 and D_2 Resonance Fine Structure Components

in Sodium and Potassium

Element	Spectral Component	Filter No.	Transmission %
^{23}Na	D_1 (5896 Å)	5940-1 5572-8	70 55
	D_2 (5890 Å)	5572-7 5840-3	73 52
^{39}K	D_1 (7699 Å)	11411 10897	68 53
	D_2 (7665 Å)	10885 10975	73 60

The observed intensity difference between σ^+ and σ^- components in sensitized fluorescence was a small fraction of the overall sensitized fluorescent intensity. The signal of the sensitized fluorescence in potassium corresponding to the polarization $(I_{\sigma^+}^{(3/2)} - I_{\sigma^-}^{(3/2)})$ was of the order of 10^{-11} A or less and thus the technique of phase-sensitive detection used with sodium (Elbel, Niewitecka and Krause, 1970) was replaced by a D.C. method using a Keithley pico-ammeter. The constant part of the signal due to the unpolarized sensitized fluorescence which was of the order 10^{-10} A, was suppressed electronically to permit accurate measurements of $(I_{\sigma^+}^{(3/2)} - I_{\sigma^-}^{(3/2)})$. For these reasons it was possible to obtain Hanle curves in sensitized fluorescence of potassium only at three pressures of helium and at one pressure of neon.

IV. DISCUSSION OF THE RESULTS

1. Hanle Effect in Resonance Fluorescence and in Sensitized Fluorescence

Figure 6 shows Hanle signals in resonance (and sensitized) fluorescence of sodium and in resonance fluorescence of potassium, in which the curves represent Eqs. (12) and (18) and the points are experimental. Figs. 7 and 8 show Hanle signals in resonance fluorescence of sodium and potassium at various helium pressures. The widths of the Hanle curves in resonance fluorescence depend on the g_J factor of the excited state and therefore the Hanle signals in D_1 resonance fluorescence are broader than in D_2 resonance fluorescence. The widths of Hanle curves in resonance fluorescence also depend on the lifetime of the excited state and this dependence causes the Hanle curves in the resonance fluorescence in sodium to be wider than in potassium. As may be seen in Figs. 7 and 8, the buffer gas pressure influences the widths of the Hanle curves in resonance fluorescence.

Although the disorientation cross section Q_D for collisions between $^2P_{3/2}$ alkali atoms and buffer gas atoms can be calculated from the widths of the Hanle curves in D_2 resonance fluorescence (Gallagher, 1967; Tudorache, 1970), the analysis of the Hanle curves shown in Figs. 6, 7 and 8

Figure 6. Hanle effect in D_2 resonance fluorescence of sodium and potassium and in sensitized fluorescence of sodium with 0.6 torr He. The points are experimental: ◊, resonance fluorescence of sodium; ●, resonance fluorescence of potassium; o, sensitized fluorescence of sodium. The solid curves were fitted to Eq. (12) and the dashed curve to Eq. (18). 1A = 9.7G.
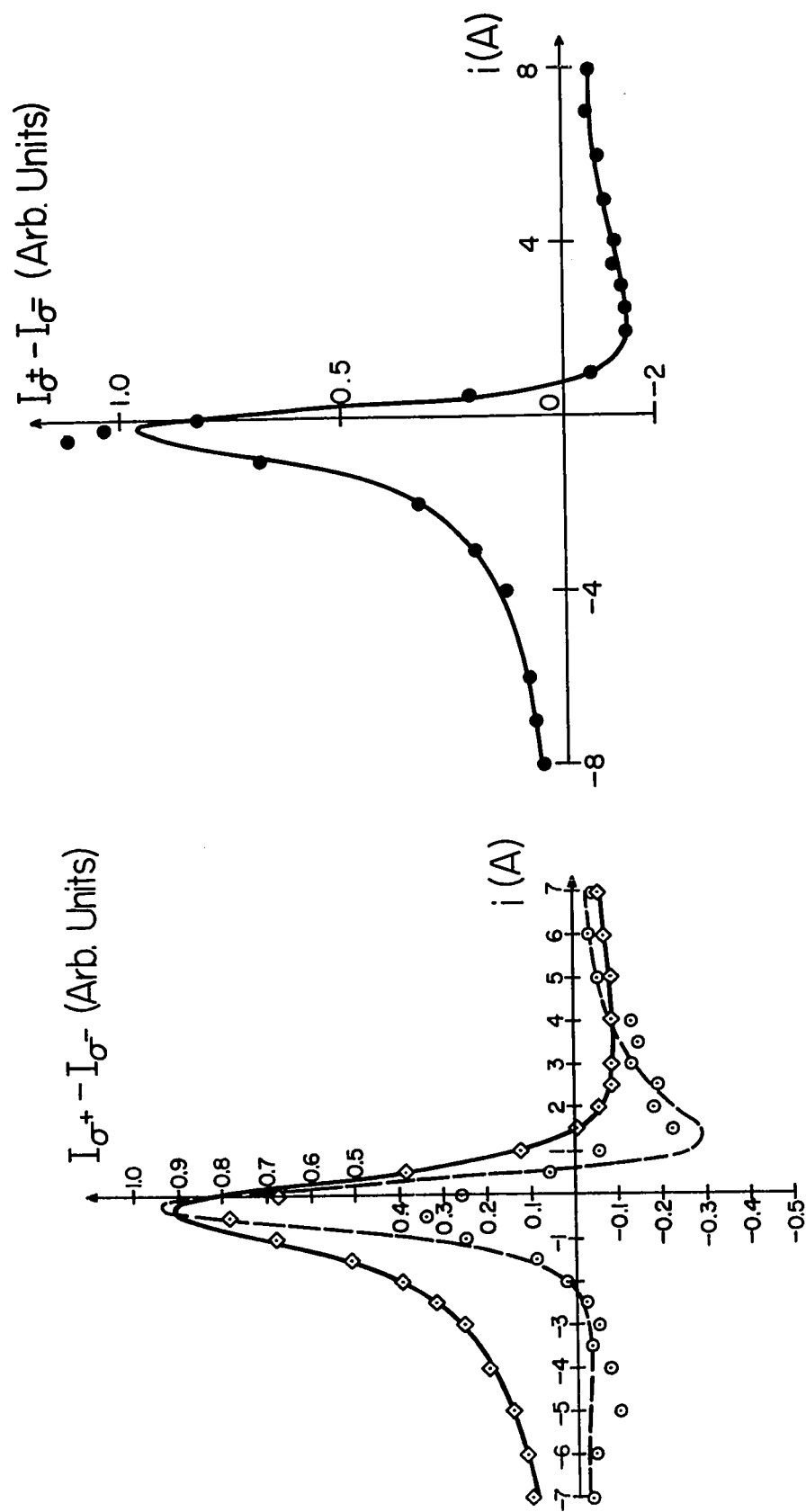
Figure 7. Hanle effect in D_1 and D_2 resonance fluorescence of sodium with various helium pressures. Dashed and continuous curves indicate D_1 and D_2 fluorescence, respectively. The points are designated as follows. For D_1 fluorescence; o, 0.56 torr; ◇, 1.28 torr; △, 1.45 torr. For D_2 fluorescence; o, 0 torr; ◇, 1.28 torr; ▽, 4.0 torr; △, 7.0 torr. 1 A ≡ 9.7 G.
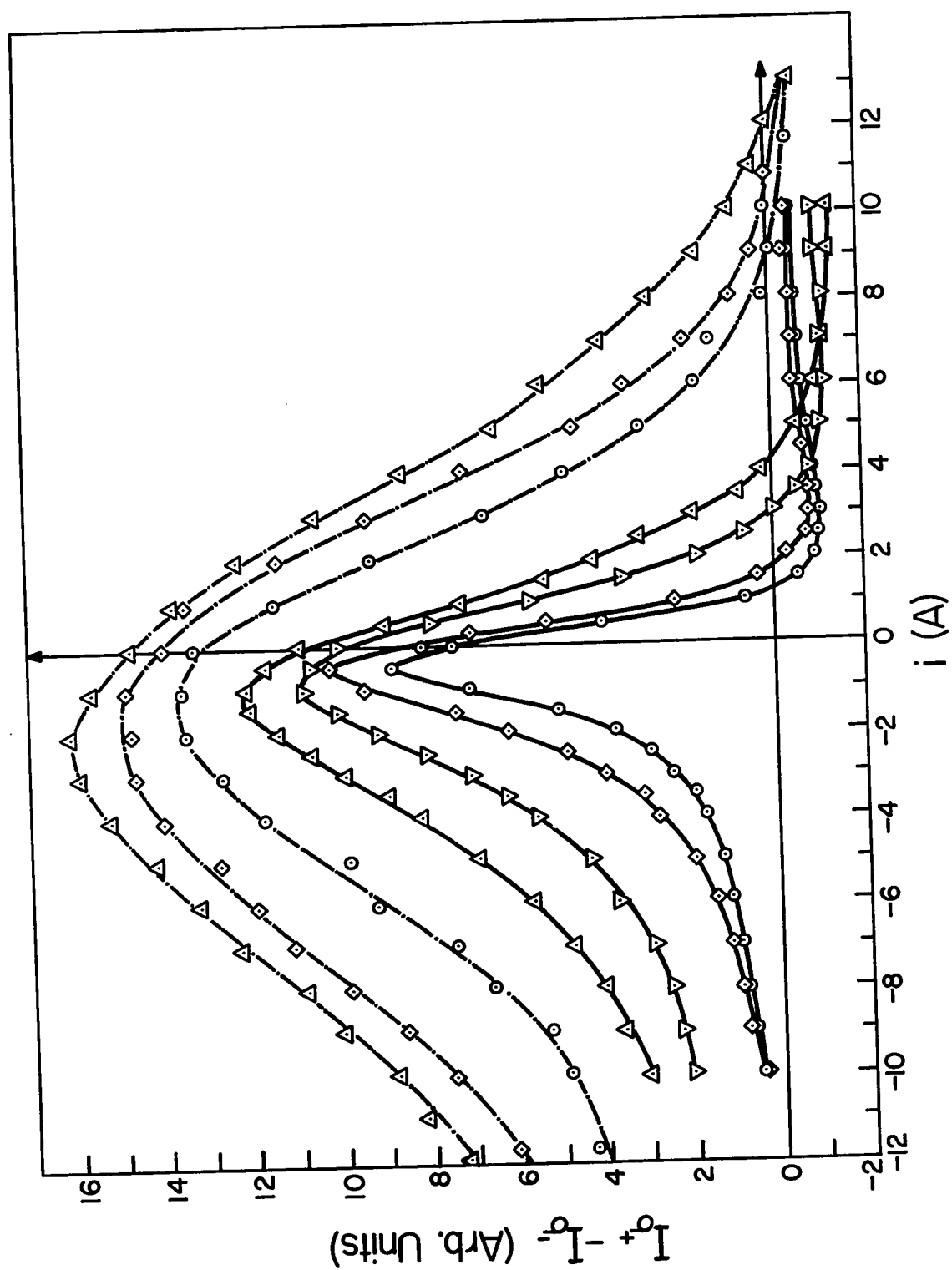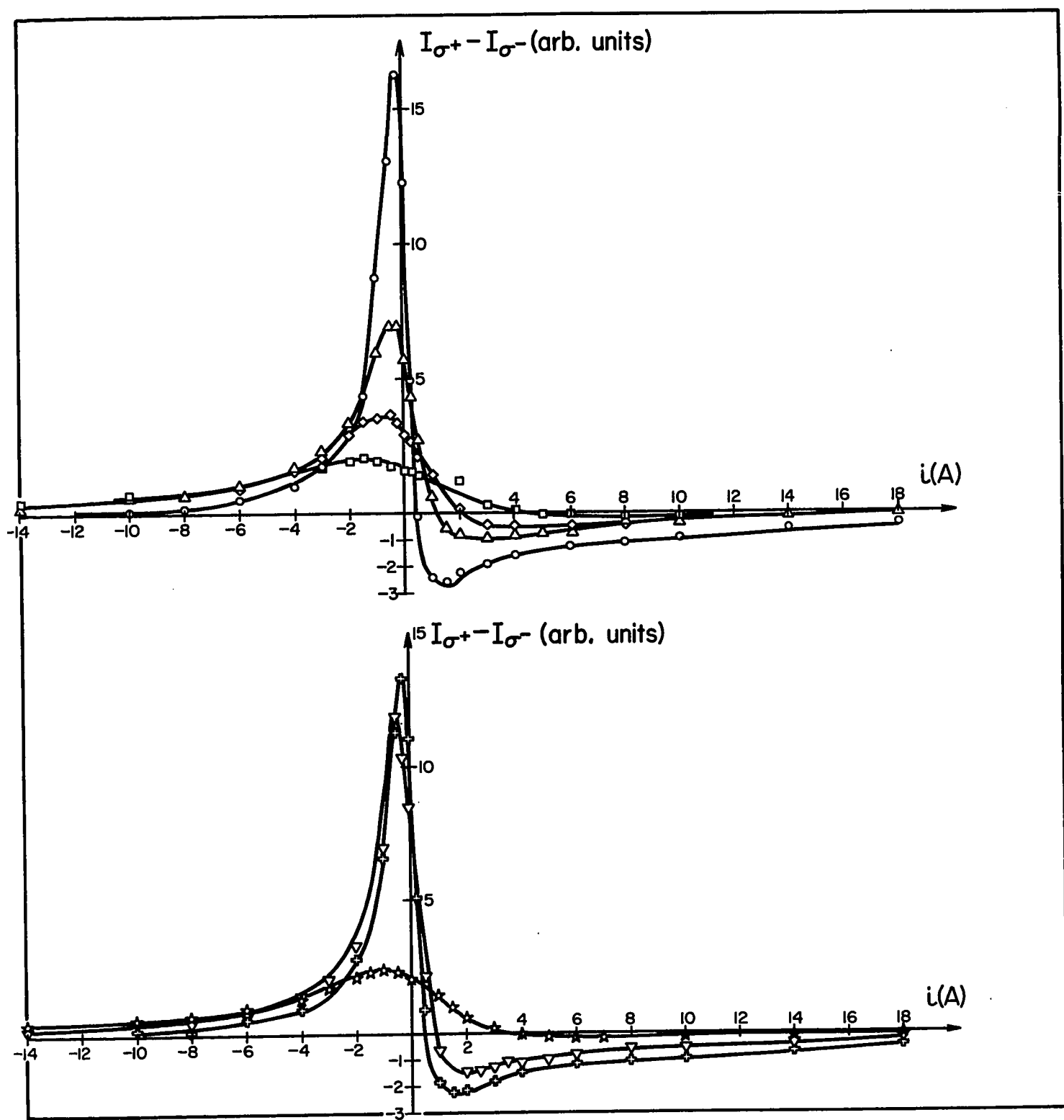
Figure 8. Hanle effect in D_2 resonance fluorescence of potassium with various helium pressures. The points are designated as follows: o, 0 torr; ✛, 0.21 torr; ∇ , 0.6 torr; △ , 1.6 torr; ◇, 3.8 torr; ✰, 6.7 torr; □ , 9.1 torr. 1 A ≡ 9.7 G.

turned out to be rather more complicated than expected.
According to Bulos and Happer (1971), nuclear spin exerts
a considerable effect on the disorientation cross section
and, in order to derive the proper results from the experi-
mental data, it is necessary to know precisely the magnetic
field strength at which the nuclear spin $\vec{I}$ becomes decoupled
from the total electronic angular momentum $\vec{J}$. For this
reason no attempt has been made to obtain values of Q_D from
the Hanle curves observed in the course of this study.
Further experimental investigations of the disorienting
collisions at various magnetic fields are now in progress
in this laboratory and should provide some clarification of
this problem.

Figure 9 shows a series of Hanle curves in sensitized
fluorescence of sodium, induced by collisions with helium
atoms at various helium pressures. Similar Hanle curves
obtained in sensitized fluorescence of potassium induced
in collisions with helium and neon atoms are shown in Fig. 10.
Fig. 11 shows a comparison between the Hanle signals observed
in resonance fluorescence and in sensitized fluorescence
of both sodium and potassium, at a helium pressure of
approximately 0.6 torr. A similar comparison is presented
in Fig. 6 except that there the points are experimental and
the curves corresponding to the resonance fluorescence have
been fitted to Eq. (12) and the curve corresponding to
sensitized fluorescence in sodium to Eq. (18). No fit to
Eq. (18) has been attempted for the Hanle effect in

Figure 9. Hanle effect in sensitized fluorescence of
sodium with various helium pressures. 1 A ≡ 9.7 G.
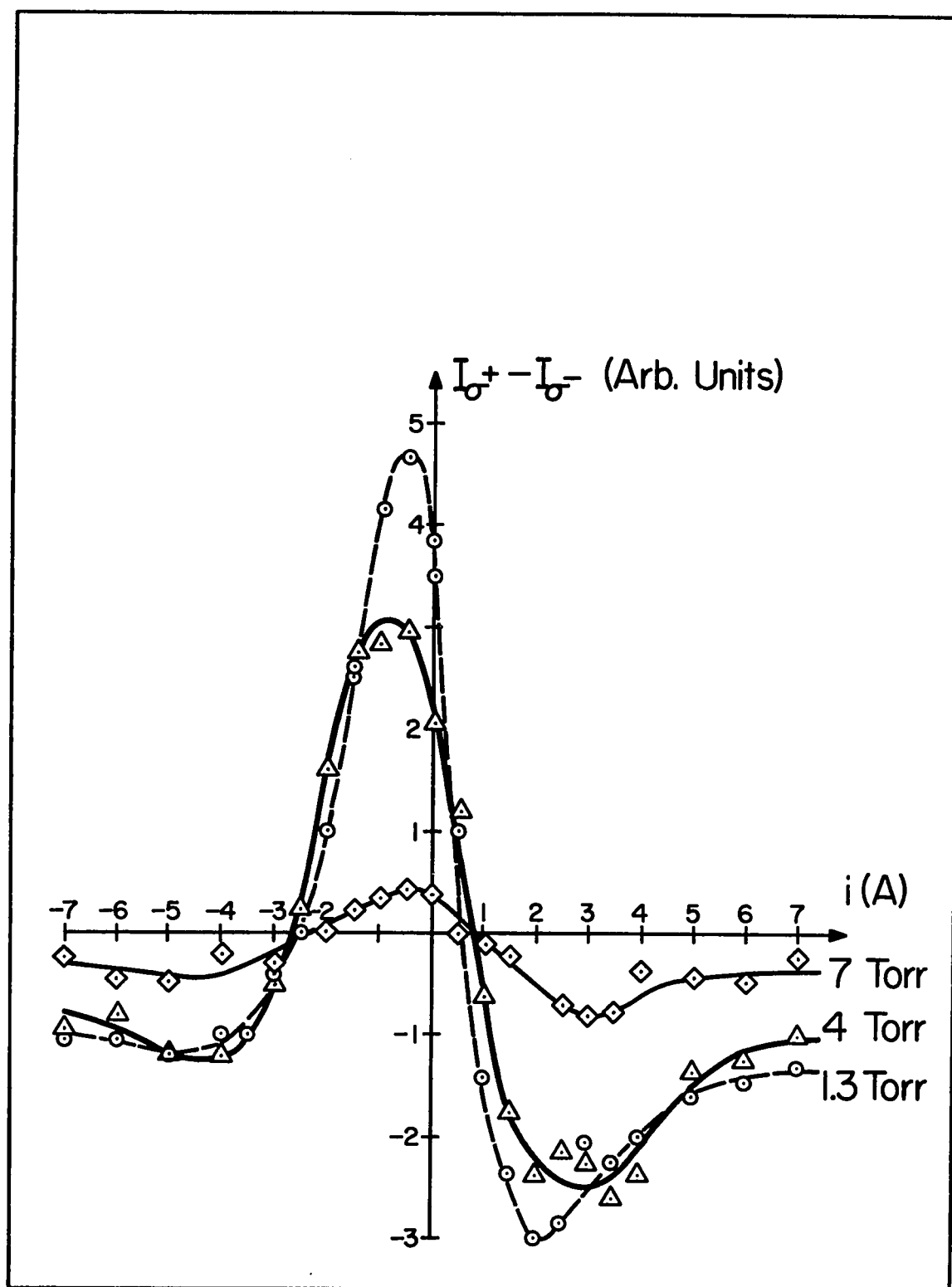
Figure 10. Hanle effect in sensitized fluorescence of potassium. o, 0.35 torr He;

△, 0.42 torr He; ◇, 0.52 torr Ne. 1 A ≡ 9.7 G.
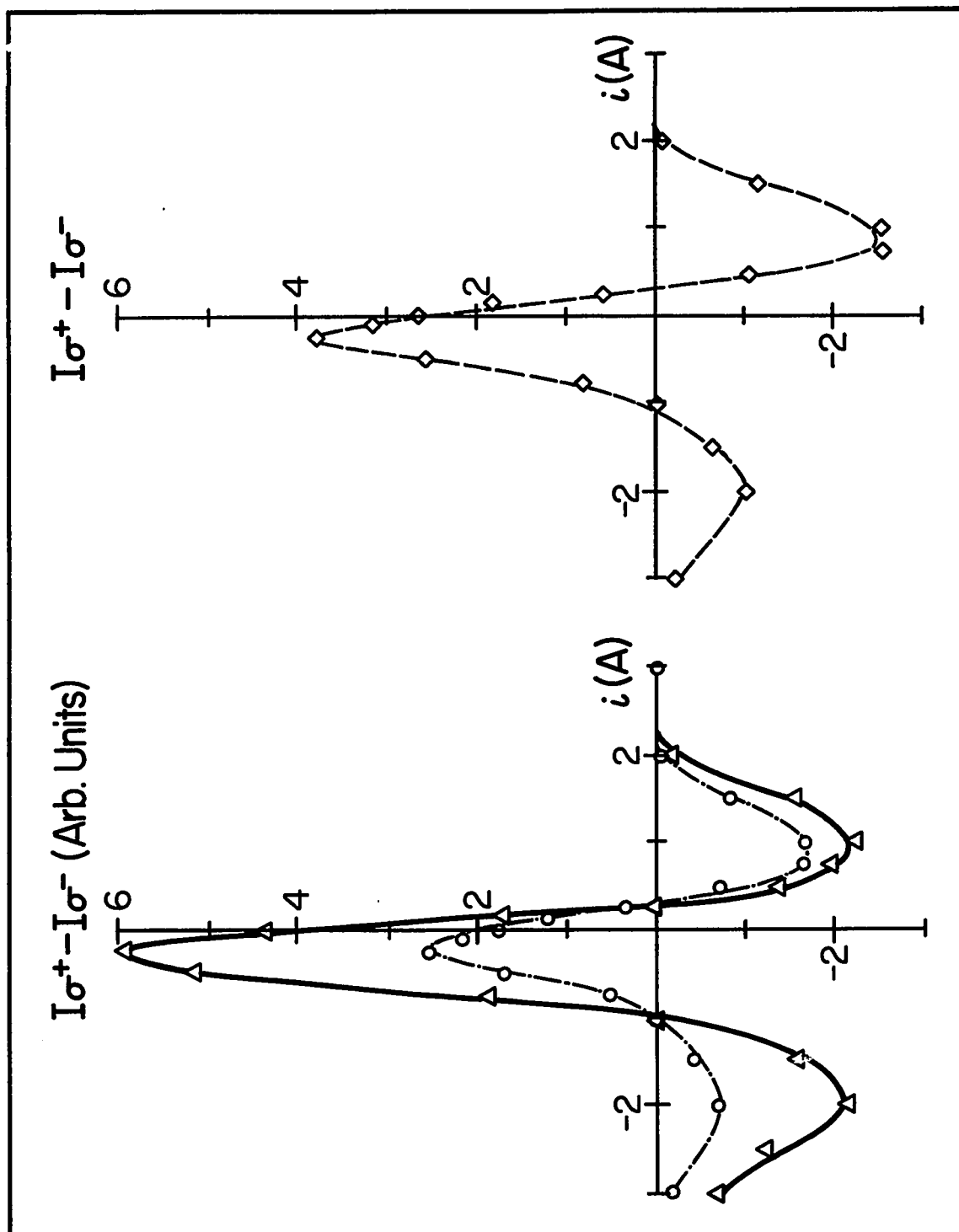
Figure 11. Comparison between Hanle signals observed in sensitized fluorescence and in resonance fluorescence of sodium and potassium. In each case the broader curve represents Hanle effect in resonance fluorescence arising from the decay of the $^2P_{3/2}$ state. 1 A $\equiv$ 9.7 G.

Potassium + 0.6 Torr He

$I_{\sigma^+} - I_{\sigma^-}$ (arb. units)

Sodium + 0.56 Torr He

$I_{\sigma^+} - I_{\sigma^-}$ (arb. units)

$i(A)$

sensitized fluorescence of potassium for reasons which will be explained below. $\omega\tau'$ was used as the adjustable parameter in Eq. (12) and the adjustable parameter in Eq. (18) was $\omega/\Omega = g_{1/2}/g_{3/2}$. The best fit to Eq. (18) was obtained by taking $g_{1/2}/g_{3/2} = 0.75$ although this value cannot be justified theoretically. The assumed numerical value of $g_{1/2}/g_{3/2}$ does not affect too seriously the shape of the Hanle curves which broaden as the ratio $g_{1/2}/g_{3/2}$ is decreased but remain always narrower than the Hanle curves in resonance fluorescence, as may be seen in Figs. 6, 7, 8, 12 and 13. Decreasing the ratio $g_{1/2}/g_{3/2}$ from 0.75 to 0.5 (which is the correct value with decoupled nuclear spin) shifts the negative intercept of the Hanle curve in Fig. 6 from −2.3 A to −2.7 A and moves it slightly away from the best fit to the experimental data.

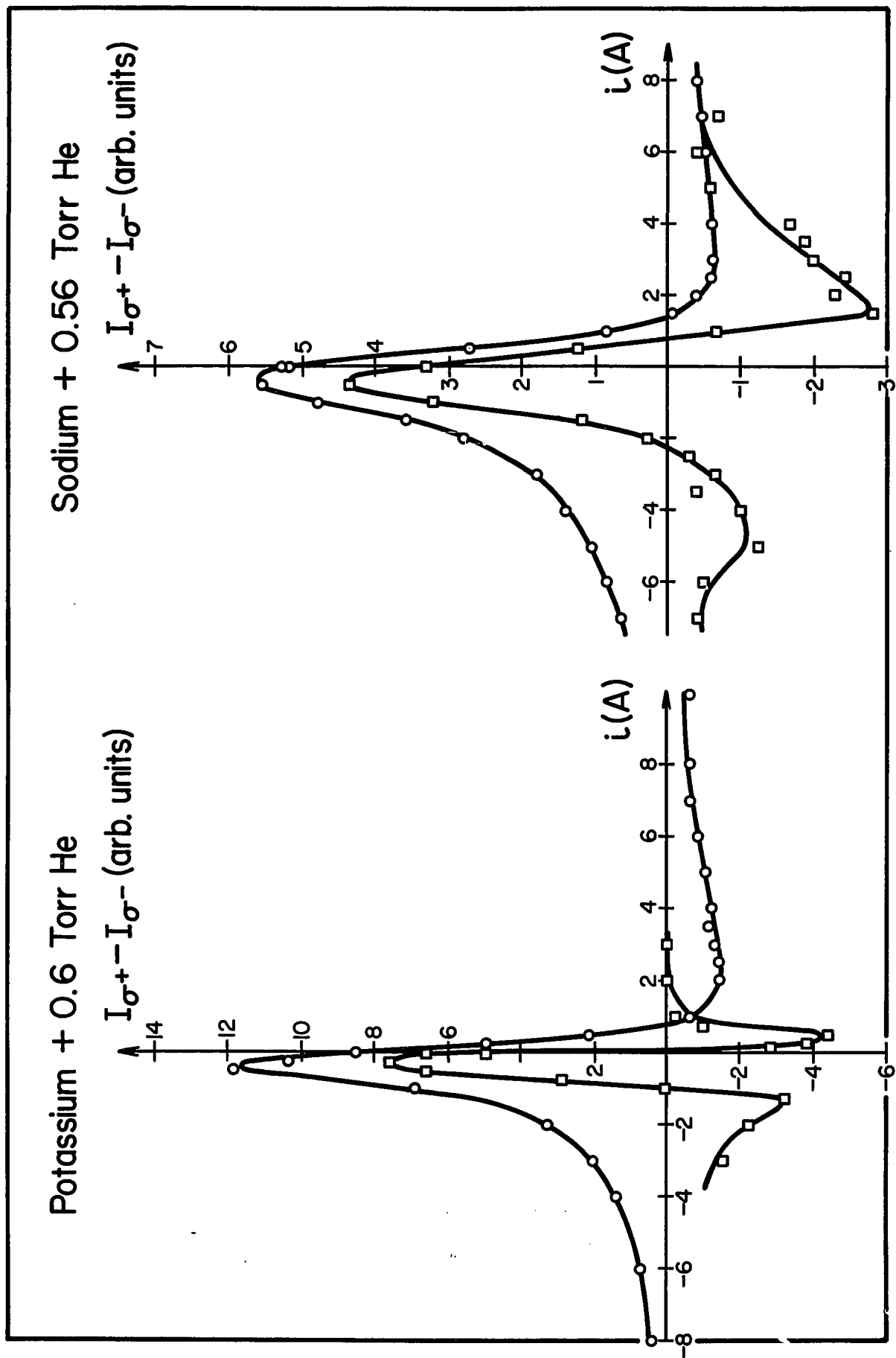It may be seen that the widths of the curves, measured between the intercepts on the abcissa, are approximately 30 G ± 15% for sodium and 12 G ± 15% for potassium. This difference in width is very likely due to differences between h.f.s. splitting in the $^2P_{3/2}$ state of sodium and of potassium (Schmieder et al, 1970).

The Hamiltonian H_o for the fine and hyperfine structure interactions in a $^2P_{3/2}$ alkali atom with nuclear spin $I = 3/2$, placed in magnetic field H, may be written as follows (Kopferman, 1958):

Figure 12. Hanle signals observed in sensitized fluorescence of sodium with helium, neon and argon. ◈ , 0.99 torr He; o, 1.08 torr Ne; △ , 0.94 torr Ar. 1 A ≡ 9.7 G.
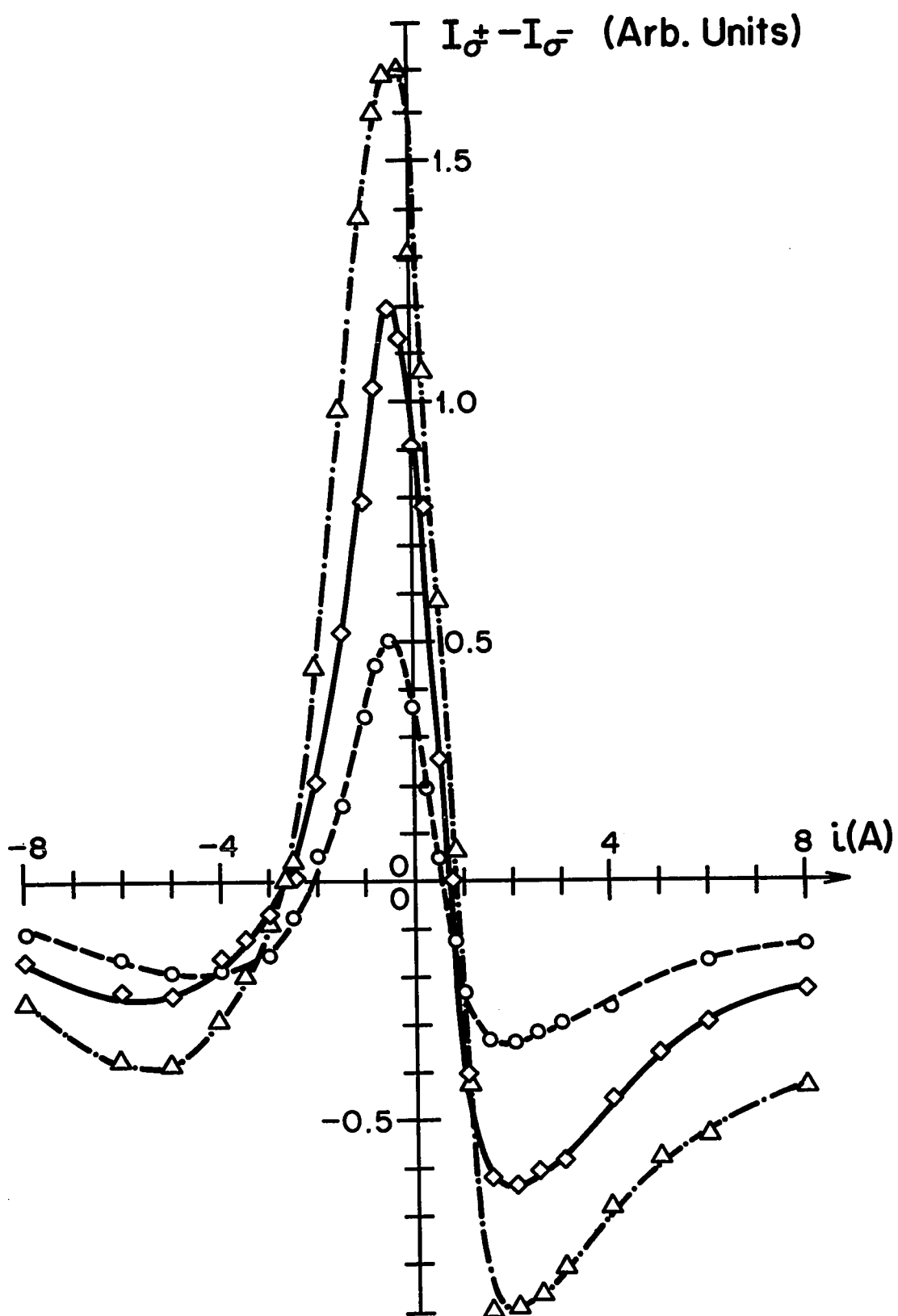
Figure 13. Hanle signals observed in sensitized
fluorescence of sodium with krypton and xenon. $\triangle$, 1 torr
Kr; o, 1.08 torr Xe. 1 A $\equiv$ 9.7 G.
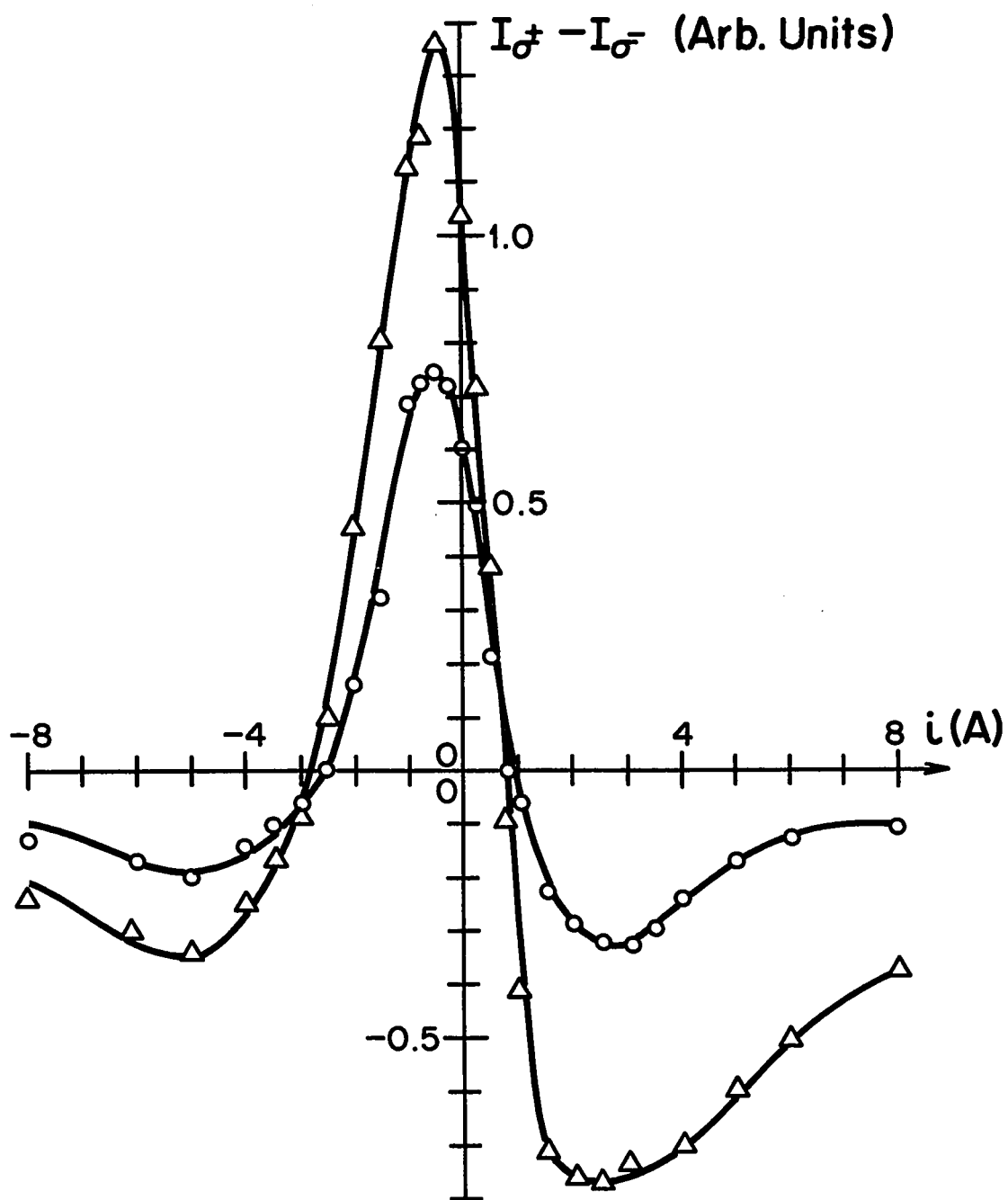
$$(37) \qquad H_o = (g_J \vec{J} - g_I \vec{I}) \cdot \mu_B \vec{H} + a\vec{I} \cdot \vec{J}$$

$$+ b \; \frac{\frac{3}{2}(IJ + \frac{1}{2})\vec{I} \cdot \vec{J} - \frac{1}{2} I^2 J^2}{I(2I + 1)(2J + 1)} \quad ,$$

where $g_J \mu_B \vec{J}$ and $g_I \mu_B \vec{I}$ are the electronic and nuclear magnetic moments, respectively, $J = 3/2$ is the total angular momentum in the $^2P_{3/2}$ state, and a and b are the electric dipole and magnetic quadrupole h.f.s. constants, respectively. The hyperfine structure constant a, which determines the hyperfine splitting equals 18.9 ± 0.3 MHz for ^{23}Na and 6.0 ± 0.1 MHz for ^{39}K (Schmieder et al, 1970). Thus it may be seen that the h.f.s. splitting in the $^2P_{3/2}$ state of potassium is approximately three times smaller than in the $^2P_{3/2}$ state of sodium while the widths of the respective Hanle signals are in the ratio of about 2.5.

Nuclear spin plays a very important role in the transfer of polarization and in the Hanle effect in sensitized fluorescence. At low magnetic fields the nuclear spin $\vec{I}$ is coupled to the electronic angular momentum $\vec{J}$ causing the predominant σ^+ polarization of the sensitized fluorescence and thus giving rise to the central peak in the Hanle curve, even though on the basis of Fig. 2 in which nuclear spin was not considered, the sensitized fluorescence might be expected to be polarized in the σ^- sense. It has been suggested that the inversion on the wings of the Hanle signal in sensitized fluorescence is

connected with the decoupling of the nuclear spin. This postulate has been verified by Elbel and Schneider (1970), who observed an inversion of the signal ($I_{\sigma^+} - I_{\sigma^-}$) in the sensitized fluorescence of sodium at a field of about 30G, at which the Hanle curves shown in Fig. 9 intercept the abcissa. The decoupling of $\vec{I}$ and $\vec{J}$ in potassium should take place at a field approximately three times lower than in sodium since the hyperfine structure constant a is also smaller by a factor of three. This is borne out by the widths of the Hanle curves in sensitized fluorescence.

As might be expected, Eq. (18) which describes Hanle effect in sensitized fluorescence gives the best fit to the experimental results in the region of decoupled nuclear spin since nuclear spin was disregarded in the derivation. The Hanle curves in sensitized fluorescence of potassium are quite narrow and their amplitudes on the "wings" rapidly approach zero, which makes it very difficult to obtain a satisfactory fit of the experimental results to Eq. (18).

There is additional experimental evidence in favour of the hypothesis that the widths of the Hanle curves in sensitized fluorescence depend only on the hyperfine structure of the $^2P_{3/2}$ state. It was found that the positions of the intercepts and thus the widths of the Hanle signals were independent of buffer gas pressure and did not vary from one gas to another, as would be expected if the decoupling of nuclear spin depends only on the magnetic

field strength but not on collisional depolarization. It

may be seen in Figs. 10, 12 and 13 that the widths of the

Hanle curves observed with various buffer gases are identical

within the limit of experimental error ($\pm$ 15%) and are

unaffected by changes in pressure.

2. <u>Cross Sections for Coherence Transfer Accompanying</u>

$^2\underline{P}_{1/2}$ - $^2\underline{P}_{3/2}$ <u>Excitation Transfer</u>

Figs. 14, 15 and 16 show plots of the ratios $V =$

$(I_{\sigma^+}^{(3/2)} - I_{\sigma^-}^{(3/2)})/(I_{\sigma^+}^{(1/2)} - I_{\sigma^-}^{(1/2)})$ for sodium and

potassium against various buffer gas pressures. At

pressures below 1.5 torr the experimental points can be

represented by a straight line and, consequently, in the

expression:

$$(38) \qquad V = \sqrt{\frac{5}{2}} \; \frac{Q_C}{Q_D + 1/\tau \, N \, v_r} \quad ,$$

which results directly from Eq. (35), Q_D may be neglected

in comparison with $1/\tau \, N \, v_r$. The validity of this approxi-

mation may be checked numerically by substituting typical

experimental values in Eq. (38). With $\tau \simeq 1 \times 10^{-8}$ s;

$v_r \simeq 1 \times 10^5$ cm/s and $N \simeq 1 \times 10^{15}$ cm^{-3} at 1 torr, $1/\tau \, N \, v_r$

$\simeq 1 \times 10^{-12}$ cm^2 as compared with $Q_D \simeq 1 \times 10^{-14}$ cm^2.

The coherence transfer cross sections obtained by

the substitution of experimental data in Eq. (35) are

listed in Table III and are compared with values obtained

by Elbel and Schneider (1971). It may be seen that Elbel's

and Schneider's values for Q_C differ by a constant factor

Figure 14. Plots of the ratios $V = (I_{\sigma^+}^{(3/2)} - I_{\sigma^-}^{(3/2)})/(I_{\sigma^+}^{(1/2)} - I_{\sigma^-}^{(1/2)})$ in sodium against He, Ne and Ar pressures.
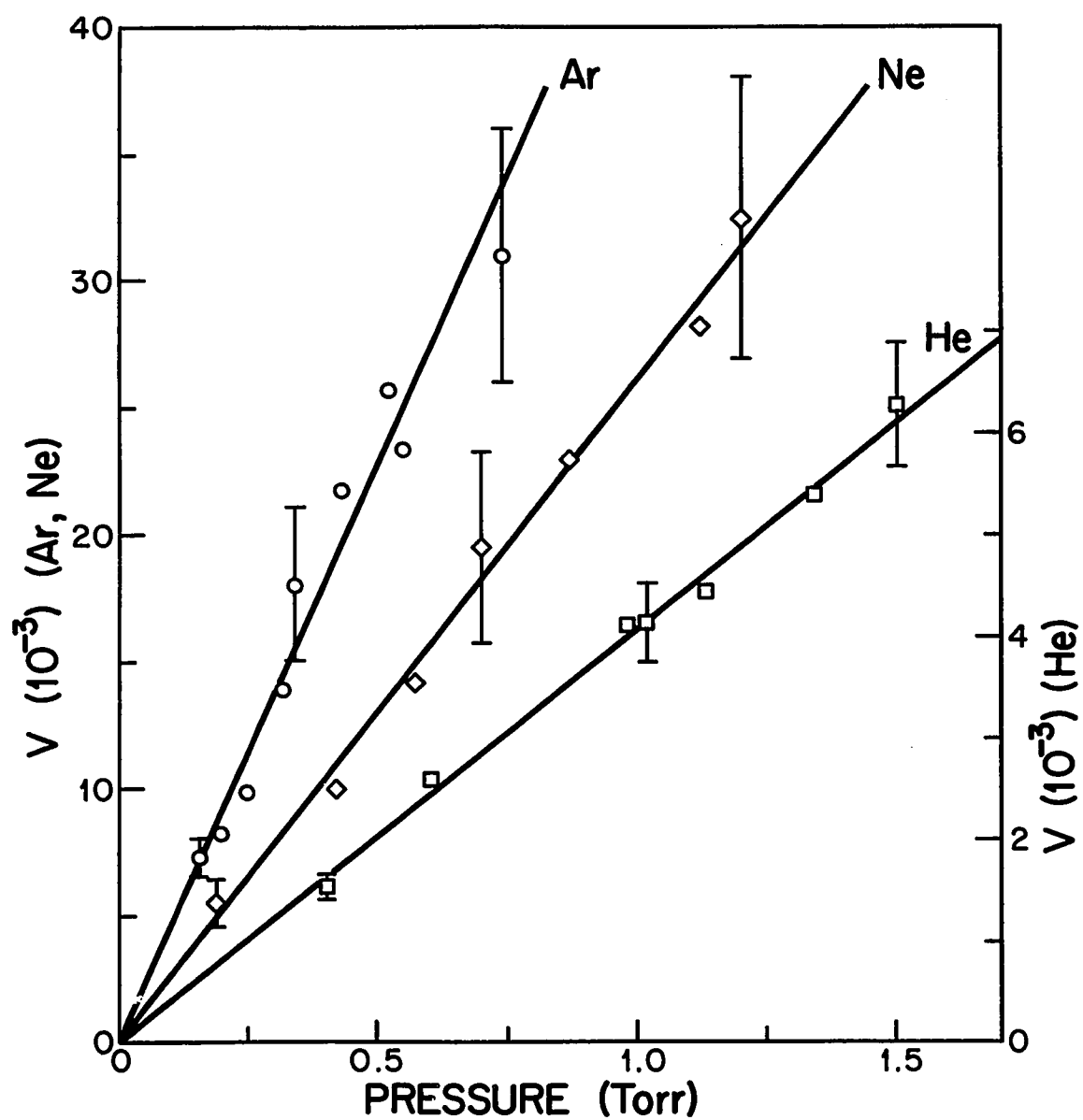
Figure 15. Plots of the ratios $V = (I_{\sigma^+}^{(3/2)} - I_{\sigma^-}^{(3/2)})/ (I_{\sigma^+}^{(1/2)} - I_{\sigma^-}^{(1/2)})$ in sodium against Kr and Xe pressures.
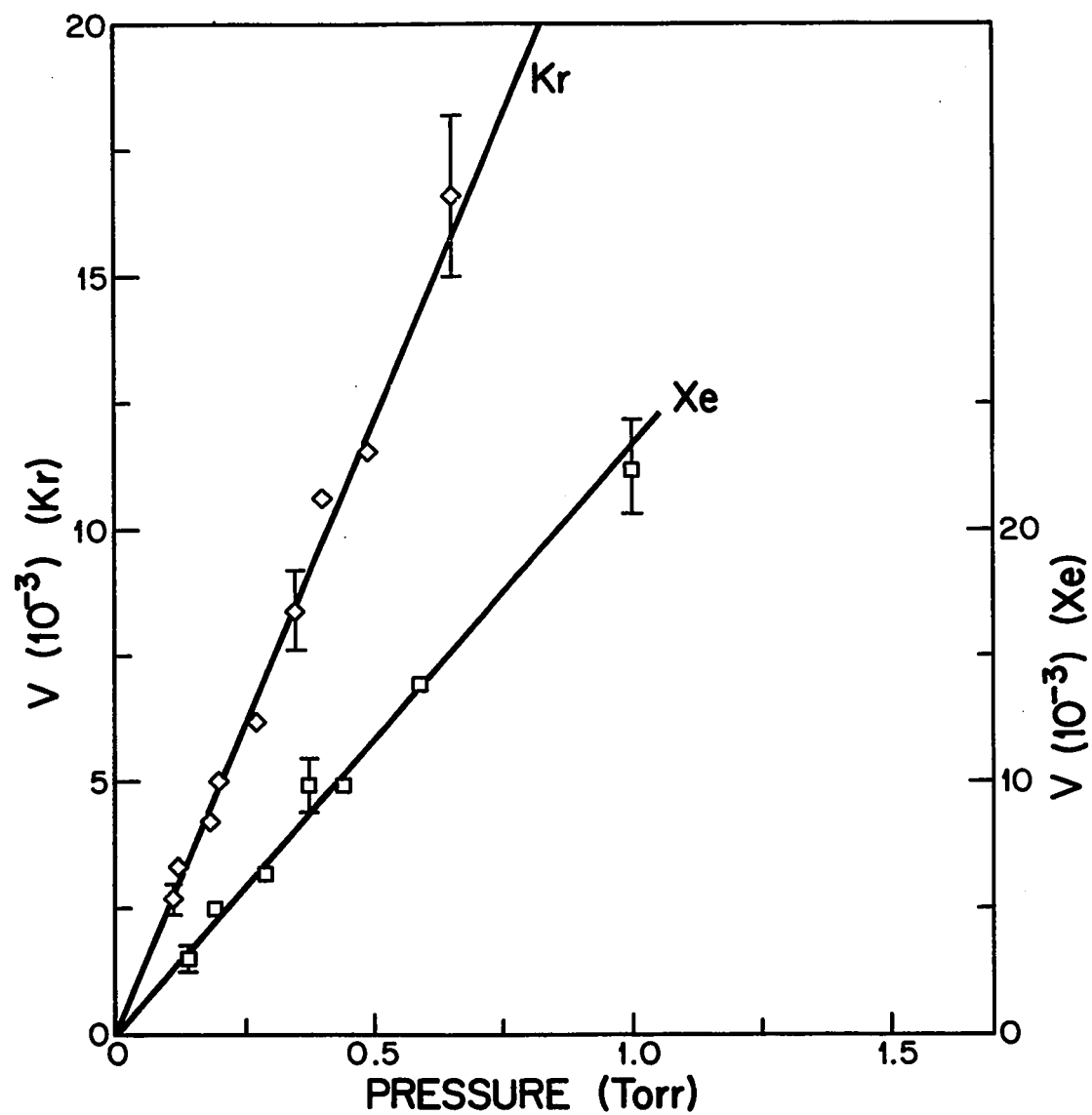
Figure 16. Plots of the ratios $V = (I_{\sigma^+}^{(3/2)} - I_{\sigma^-}^{(3/2)})/$ $(I_{\sigma^+}^{(1/2)} - I_{\sigma^-}^{(1/2)})$ in potassium against the pressures of various buffer gases.
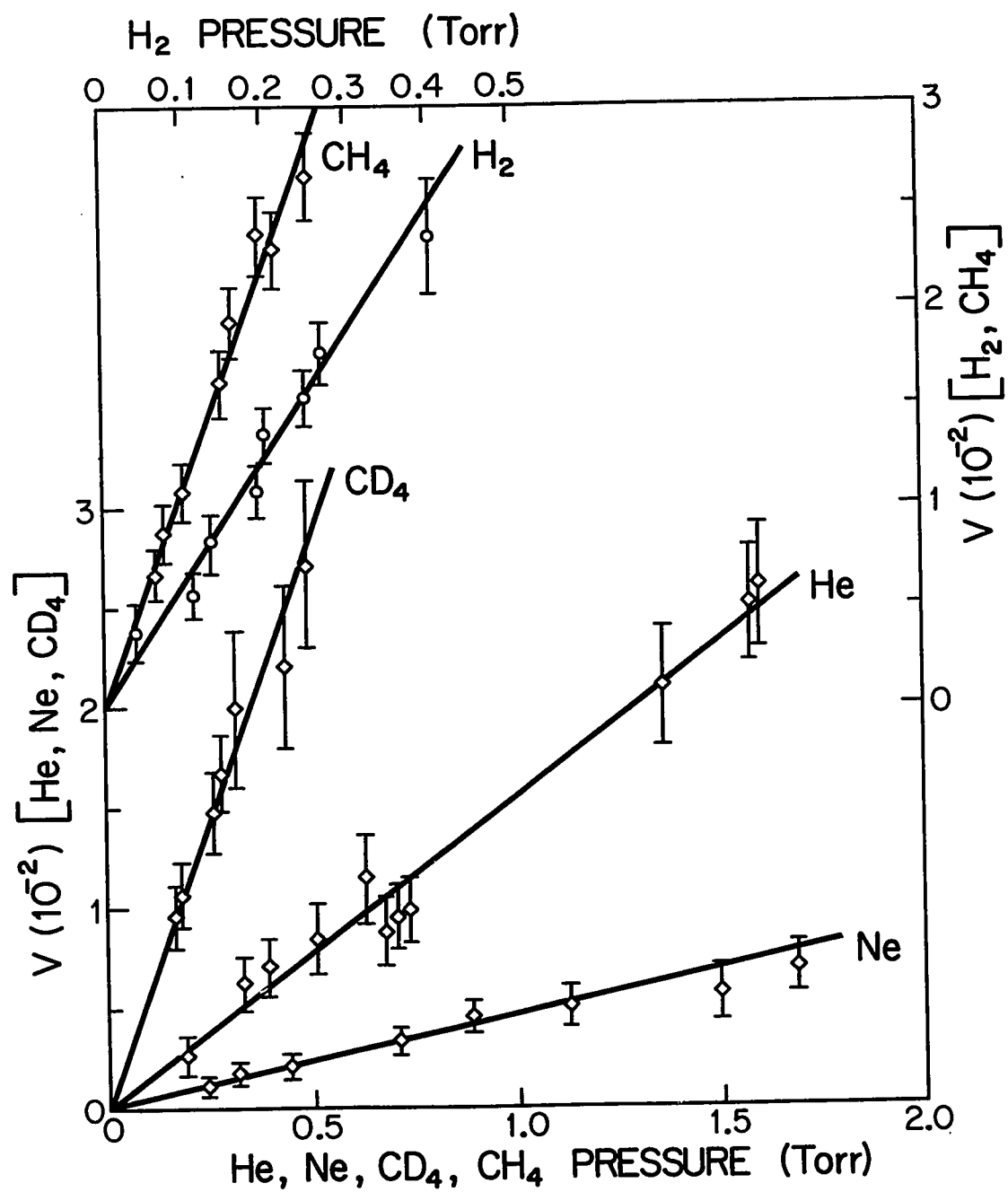
TABLE III

Cross Sections for Coherence Transfer Accompanying
$^2P_{1/2} - {}^2P_{3/2}$ Excitation Transfer in Sodium and Potassium,
Induced by Collisions with Various Buffer Gases

Collision Partners	Present Investigation Q_C ($\mathring{A}^2$)	Elbel and Schneider (a) Q_C ($\mathring{A}^2$)	$^2P_{1/2} \rightarrow {}^2P_{3/2}$ Mixing Cross Sections ($\mathring{A}^2$)
Na - He	7.1 ± 0.7	22 ± 4.4	86 (b)
Na - Ne	6.2 ± 0.6	24 ± 4.8	67 (b)
Na - Ar	12.0 ± 1.2	26 ± 5.2	110 (b)
Na - Kr	6.8 ± 0.7	20 ± 4.0	90 (b)
Na - Xe	6.9 ± 0.7	23 ± 4.6	85 (b)
K - He	1.7 ± 0.4	-	56.5 (c)
K - Ne	0.8 ± 0.1	-	14.3 (c)
K - Ar	< 0.5	-	36.7 (c)
K - H_2	3.5 ± 0.7	-	76.0 (c)
K - CH_4	7 ± 0.6	-	-
K - CD_4	7.7 ± 0.5	-	-

(a) Elbel and Schneider (1971)

(b) Pitre and Krause (1967)

(c) Chapman and Krause (1966)

(d) McGillis and Krause (1968)

from the results of this investigation. It is suggested
that this discrepancy is due to a difference in a numerical
factor which appears in the equation used to obtain Q_C from
the experimental data. Elbel and Schneider (1971) calculated
their cross section Q_C from the following equation.

$$(39) \quad Q_C = 2 \frac{I_{\sigma^+}^{(3/2)} - I_{\sigma^-}^{(3/2)}}{I_{\sigma^+}^{(1/2)} - I_{\sigma^-}^{(1/2)}} \left[Q_D + \frac{1}{\tau N v_r} \right]$$

which differs from Eq. (35) by the numerical factor $\sqrt{10}$.
Elbel and Schneider used the following expression for the
polarization ratio:

$$(40) \quad \frac{I_{\sigma^+}^{(3/2)} - I_{\sigma^-}^{(3/2)}}{I_{\sigma^+}^{(1/2)} - I_{\sigma^-}^{(1/2)}} = \frac{1}{2} \frac{\langle J_z \rangle_{3/2}}{\langle J_z \rangle_{1/2}}$$

which appears to be incorrect. This can be verified by
calculating the polarization $\langle J_z \rangle_J$ in the $|J\rangle$ state.

$$(41) \quad \langle J_z \rangle_J = \frac{\sum_{m_J} m_J N_{m_J}^J}{N_o^J}$$

where $N_{m_J}^J$ was defined previously and $N_o^J = \sum_{m_J} N_{m_J}^J$. Since

$$(42) \quad I_{\sigma^\pm}^{(3/2)} \propto 3 N_{\pm 3/2}^{(3/2)} + N_{\pm 1/2}^{(3/2)} \quad \text{and}$$

$$I_{\sigma^\pm}^{(1/2)} \propto 2 N_{\pm 1/2}^{(1/2)}$$

the ratio of polarizations should be

$$(43) \quad \frac{I_{\sigma+}(3/2) - I_{\sigma-}(3/2)}{I_{\sigma+}(1/2) - I_{\sigma-}(1/2)} = \frac{1}{2} \frac{N_o(3/2)}{N_o(1/2)} \frac{\langle J_z \rangle_{(3/2)}}{\langle J_z \rangle_{(1/2)}}$$

The ratio $N_o(3/2)/N_o(1/2)$ is not equal to unity as seems to have been assumed by Elbel and Schneider (1971). For example, for excitation with an ideal spectral lamp ($I_{D_1} = 1/2 \, I_{D_2}$), $N_o(3/2) = 4N_o(1/2)$, and for excitation with white light ($I_{D_1} = I_{D_2}$), $N_o(3/2) = 2N_o(1/2)$. However, on applying Eq. (35) to Elbel and Schneider's (1971) results, good agreement is obtained between the two sets of cross sections[*].

Some qualitative conclusions can be drawn from a comparison of the coherence transfer cross section in alkali atoms with the $^2P_{1/2} \longrightarrow {}^2P_{3/2}$ mixing cross sections. The values Q_C are larger for sodium-noble gas collisions than for potassium-noble gas collisions, as are the mixing cross sections, probably because the fine structure splitting in potassium (57 cm^{-1}) is over three times larger than in sodium (17 cm^{-1}). Somewhat surprisingly, the cross sections for coherence transfer induced in collisions between potassium and molecular gases are relatively large and are larger than for alkali-noble gas collisions. The large size

---

[*]   According to a recent (private) communication from Dr. Elbel, Elbel and Schneider used the following definition of the polarization in the $|J\rangle$ state:

$$\langle J_z \rangle_J = \sum_{m_J} m_J N_{m_J}^J \quad ,$$

which differs from Eq. (41). This difference fully accounts for the apparent discrepancy between the two sets of experimental results.

of these cross sections may be an indication that $^2P_{1/2} \rightarrow$ $^2P_{3/2}$ mixing proceeds at least in part by way of sudden collisions and does not involve to any great extent the formation of a long-lived intermediate complex. If the latter were the case, the orientation of the alkali atom would be completely destroyed during the lifetime of the complex.

The present investigation may be considered as a first attempt to study the process of coherence transfer within the same atomic species (sodium and potassium), induced by collisions with atomic and molecular buffer gases. In rubidium and in cesium, the large energy defect between ^2P states (238 cm^{-1} and 554 cm^{-1}, respectively) makes the investigation of coherence transfer virtually impossible because of the exceedingly faint Hanle signal. It may, however, be possible to observe and investigate the coherence transfer between the 6^3P_1 mercury atoms and various (9S, 8D, 8P, 8S and 7S) states in sodium. The results of such an experiment, together with those obtained in the present study, should lead to more general conclusions concerning the dependence of coherence transfer cross sections on the energy defect between the atomic states involved and on the properties of the states themselves.

APPENDIX A

EXPERIMENTAL DATA

The following are the raw experimental results. The
intensities of the σ^+ and σ^- components in resonance fluor-
escence and in sensitized fluorescence represent readings
obtained with a picoammeter. The data have been corrected
for transmissions of filters, quarter-wave plates and
polarizers. Intensity differences $(I_{\sigma^+} - I_{\sigma^-})$ are given
in units of 10^{-10} A.

Na-He DATA

Pressure (torr)	$I_{\sigma^+}^{(3/2)} - I_{\sigma^-}^{(3/2)}$ (10^{-10} A)	$I_{\sigma^+}^{(1/2)} - I_{\sigma^-}^{(1/2)}$ (10^{-10} A)	$V = (I_{\sigma^+}^{(3/2)} - I_{\sigma^-}^{(3/2)})/(I_{\sigma^+}^{(1/2)} - I_{\sigma^-}^{(1/2)})$ (10^{-2})
0.4	6.40	413.0	1.55
0.6	9.76	375.2	2.60
0.98	14.31	349.0	4.10
1.02	14.15	341.0	4.15
1.13	14.66	330.2	4.44
1.34	17.40	319.8	5.44
1.50	19.93	313.9	6.35

Na-Ne DATA

Pressure (torr)	$I_{\sigma^+}^{(3/2)} - I_{\sigma^-}^{(3/2)}$ (10^{-10} A)	$I_{\sigma^+}^{(1/2)} - I_{\sigma^-}^{(1/2)}$ (10^{-10} A)	$V = (I_{\sigma^+}^{(3/2)} - I_{\sigma^-}^{(3/2)})/(I_{\sigma^+}^{(1/2)} - I_{\sigma^-}^{(1/2)})$ (10^{-2})
0.19	1.38	250.2	0.55
0.42	2.35	234.8	1.00
0.57	3.19	224.9	1.42
0.70	4.12	211.4	1.95
0.87	4.76	206.8	2.30
1.12	5.67	200.5	2.83
1.20	6.44	198.2	3.25

Na-Ar DATA

Pressure (torr)	$I_{\sigma^+}^{(3/2)} - I_{\sigma^-}^{(3/2)}$ (10^{-10} A)	$I_{\sigma^+}^{(1/2)} - I_{\sigma^-}^{(1/2)}$ (10^{-10} A)	$V = (I_{\sigma^+}^{(3/2)} - I_{\sigma^-}^{(3/2)})/(I_{\sigma^+}^{(1/2)} - I_{\sigma^-}^{(1/2)})$ (10^{-2})
0.16	1.94	262.4	0.74
0.20	2.12	255.2	0.83
0.25	2.50	250.1	1.00
0.315	3.45	248.2	1.39
0.34	4.28	237.6	1.80
0.43	4.61	212.3	2.17
0.52	5.39	208.9	2.58
0.55	5.13	219.3	2.34
0.74	5.71	183.6	3.11

Na-Kr DATA

Pressure (torr)	$I_{\sigma^+}^{(3/2)} - I_{\sigma^-}^{(3/2)}$ (10^{-10} A)	$I_{\sigma^+}^{(1/2)} - I_{\sigma^-}^{(1/2)}$ (10^{-10} A)	$V = (I_{\sigma^+}^{(3/2)} - I_{\sigma^-}^{(3/2)})/(I_{\sigma^+}^{(1/2)} - I_{\sigma^-}^{(1/2)})$ (10^{-2})
0.11	0.52	191.1	0.27
0.12	0.62	187.3	0.33
0.18	0.74	177.3	0.42
0.20	0.85	170.8	0.50
0.28	1.02	164.7	0.62
0.35	1.34	158.8	0.84
0.41	1.61	151.6	1.06
0.51	1.64	142.2	1.15
0.65	2.26	136.5	1.66

Na-Xe DATA

Pressure (torr)	$I_{\sigma^+}^{(3/2)} - I_{\sigma^-}^{(3/2)}$ $(10^{-10} A)$	$I_{\sigma^+}^{(1/2)} - I_{\sigma^-}^{(1/2)}$ $(10^{-10} A)$	$V = (I_{\sigma^+}^{(3/2)} - I_{\sigma^-}^{(3/2)})/(I_{\sigma^+}^{(1/2)} - I_{\sigma^-}^{(1/2)})$ (10^{-2})
0.09	0.52	214.7	0.24
0.14	0.56	186.8	0.30
0.19	0.82	164.3	0.50
0.29	0.92	146.2	0.63
0.37	1.01	106.3	0.95
0.44	1.05	110.5	0.95
0.59	1.41	101.2	1.39
1.00	2.15	96.0	2.24

K – He DATA

Pressure (torr)	$I_{\sigma^+}^{(3/2)} - I_{\sigma^-}^{(3/2)}$ (10^{-10} A)	$I_{\sigma^+}^{(1/2)} - I_{\sigma^-}^{(1/2)}$ (10^{-10} A)	$V = (I_{\sigma^+}^{(3/2)} - I_{\sigma^-}^{(3/2)})/(I_{\sigma^+}^{(1/2)} - I_{\sigma^-}^{(1/2)})$ (10^{-2})
0.19	0.32	123.1	0.26
0.33	0.48	75.5	0.63
0.39	0.54	76.5	0.70
0.51	0.52	61.9	0.84
0.63	0.64	55.2	1.16
0.68	0.48	54.5	0.88
0.71	0.52	54.2	0.96
0.74	0.52	51.1	0.98
1.36	0.56	26.9	2.10
1.58	0.60	23.8	2.52
1.60	0.60	23.1	2.60

K – Ne DATA

Pressure (torr)	$I_{\sigma^+}^{(3/2)} - I_{\sigma^-}^{(3/2)}$ (10^{-10} A)	$I_{\sigma^+}^{(1/2)} - I_{\sigma^-}^{(1/2)}$ (10^{-10} A)	$V = (I_{\sigma^+}^{(3/2)} - I_{\sigma^-}^{(3/2)})/(I_{\sigma^+}^{(1/2)} - I_{\sigma^-}^{(1/2)})$ (10^{-2})
0.24	0.22	202.4	0.11
0.31	0.40	214.5	0.18
0.44	0.47	212.5	0.22
0.71	0.67	196.9	0.34
0.89	0.82	179.4	0.46
1.13	0.94	179.8	0.52
1.5	0.95	169.2	0.56
1.69	1.14	167.7	0.68

K – CH$_4$ DATA

Pressure (torr)	$I_{\sigma^+}^{(3/2)} - I_{\sigma^-}^{(3/2)}$ $(10^{-10}$ A$)$	$I_{\sigma^+}^{(1/2)} - I_{\sigma^-}^{(1/2)}$ $(10^{-10}$ A$)$	$V = (I_{\sigma^+}^{(3/2)} - I_{\sigma^-}^{(3/2)})/(I_{\sigma^+}^{(1/2)} - I_{\sigma^-}^{(1/2)})$ (10^{-2})
0.13	1.24	194.2	0.64
0.15	1.66	189.1	0.88
0.20	1.96	181.2	1.08
0.30	2.54	176.2	1.44
0.32	2.48	155.0	1.60
0.39	3.36	141.2	2.38
0.43	3.08	134.9	2.28
0.50	3.44	129.2	2.66

K - CD$_4$ DATA

Pressure (torr)	$I_{\sigma^+}^{(3/2)} - I_{\sigma^-}^{(3/2)}$ (10^{-10} A)	$I_{\sigma^+}^{(1/2)} - I_{\sigma^-}^{(1/2)}$ (10^{-10} A)	$V = (I_{\sigma^+}^{(3/2)} - I_{\sigma^-}^{(3/2)})/(I_{\sigma^+}^{(1/2)} - I_{\sigma^-}^{(1/2)})$ (10^{-2})
0.17	2.52	262.0	0.96
0.18	2.73	257.8	1.06
0.26	3.49	242.1	1.44
0.28	3.94	234.8	1.68
0.31	4.59	229.4	2.00
0.44	4.49	204.1	2.20
0.49	5.04	186.5	2.70

K – H_2 DATA

Pressure (torr)	$I_{\sigma^+}^{(3/2)} - I_{\sigma^-}^{(3/2)}$ (10^{-10} A)	$I_{\sigma^+}^{(1/2)} - I_{\sigma^-}^{(1/2)}$ (10^{-10} A)	$V = (I_{\sigma^+}^{(3/2)} - I_{\sigma^-}^{(3/2)})/(I_{\sigma^+}^{(1/2)} - I_{\sigma^-}^{(1/2)})$ (10^{-2})
0.05	0.88	220.2	0.40
0.11	1.08	196.6	0.55
0.14	1.57	187.1	0.84
0.19	1.92	177.3	1.08
0.20	2.49	180.4	1.38
0.25	2.46	160.7	1.53
0.27	2.69	161.5	1.67
0.42	3.24	139.5	2.32

BIBLIOGRAPHY

Ackermann, H. and Weber, E. 1968. Proc. Int. Conf. on Optical
        Pumping and Atomic Line Shapes (OPALS), (Państwowe
        Wydawnictwo Naukowe, Warsaw).

Bulos, R. B. and Happer, W. 1971. Phys. Rev. $\underline{4A}$, 849.

Berdowski, W., Shiner, T. and Krause, L. 1971. Phys. Rev.
        $\underline{4A}$, 984.

Breit, G. 1933. Rev. Mod. Phys. $\underline{5}$, 91.

Byron, F. W. and Foley, H. M. 1964. Phys. Rev. A. $\underline{134}$, 625.

Callaway, J. and Bauer, E. 1965. Phys. Rev. A. $\underline{140}$, 1072.

Chapman, G. D. 1965. Ph.D. Thesis, University of Windsor.

Chapman, G. D. and Krause, L. 1966. Can. J. Phys. $\underline{44}$, 753.

Cheron, B. and Barrat, J. P. 1968. C. R. Acad. Sci. Paris,
        $\underline{B266}$, 1324.

Chiu, L. Y. C. 1972. Phys. Rev. $\underline{5A}$, 2053.

Copley, G. and Krause, L. 1969. Can. J. Phys. $\underline{47}$, 533.

D'yakonov, M. I. and Perel', V. I. 1965. Sov. Phys. J.E.T.P.
        $\underline{20}$, 997.

Elbel, M. and Naumann, F. 1967a. Z. Phys. $\underline{204}$, 501.

Elbel, M. and Naumann, F. 1967b. Z. Phys. $\underline{208}$, 104.

Elbel, M. and Schneider, W. 1968. Proc. Int. Conf. on Optical
        Pumping and Atomic Line Shapes (OPALS), (Państwowe
        Wydawnictwo Naukowe, Warsaw).

Elbel, M., Niewitecka, B. and Krause, L. 1970. Can. J. Phys.
        $\underline{48}$, 2996.

Elbel, M. 1970. Can. J. Phys. $\underline{48}$, 3047.

Elbel, M. and Schneider, W. 1970. Phys. Verh. $\underline{5}$, 362.

Elbel, M. and Schneider, W. 1971. Z. Phys. $\underline{241}$, 244.

Fano, U. 1957. Rev. Mod. Phys. 29, 74.

Franz, F. A. and Franz, J. R. 1966. Phys. Rev. 148, 82.

Franz, F. A. 1969. Phys. Lett. 29A, 326.

Franzen, W. 1959. Phys. Rev. 115, 850.

Fricke, J., Haas, J., Lüscher, E. and Franz, F. A. 1967.
    Phys. Rev. 163, 45.

Gallagher, A. 1967. Phys. Rev. 157, 68.

Gordeyev, E. P., Nikitin, E. E. and Ovchinnikova, M. Ya.
    1969. Can. J. Phys. 47, 1819.

Gough, W. 1967. Proc. Phys. Soc. 90, 287.

Grawert, G. 1969. Z. Phys. 225, 283.

Guiry, J. and Krause, L. 1972. Phys. Rev. 6A, 273.

Hanle, W. 1927. Z. Phys. 41, 164.

Happer, W. 1972. Rev. Mod. Phys. 44, 169.

Kibble, B. P., Copley, G. and Krause, L. 1967. Phys. Rev.
    153, 9.

Kopferman, H. 1958. Nuclear Moments, (Academic Press Inc.,
    New York).

Kraulinya, E. E. Sametis, O. S. and Bryukhovetskii, A. P.
    1970, Opt. Spectry. 29, 227.

McGillis, D. A. and Krause, L. 1968. Can. J. Phys. 46, 25.

Niewitecka, B. and Krause, L. 1973. Can. J. Phys. (to be
    published).

Omont, A. 1965. J. Physique 26, 26.

Papp, J. F. and Franz, F. A. 1972. Phys. Rev. 5A, 1763.

Pitre, J. and Krause, L. 1967. Can. J. Phys. 45, 2671.

Sametis, O. S. and Kraulinya, E. K. 1969. Sensitized
    Fluorescence of Mixtures of Metal Vapours, Vol. 1,
    (Riga).

Series, G. W. 1967. Proc. Phys. Soc. 90, 1179.

Schmieder, R. W., Lurio, A., Happer, W. and Khadjavi, A. 1967. Phys. Rev. $\underline{2A}$, 1216.

Schneider, W. 1971. Z. Phys. $\underline{248}$, 387.

Schearer, L. D. and Riseberg, L. A. 1971. Phys. Rev. Lett. $\underline{26}$, 596.

Stupavsky, M. and Krause, L. 1969. Can. J. Phys. $\underline{47}$, 1249.

Tudorache, S. 1970. Rev. Roum. Phys. $\underline{15}$, 269.

Wang, C. H. and Tomlinson, W. J. 1969. Phys. Rev. $\underline{181}$, 115.

Zhitnikov, R. A., Kuleshov, P. P. and Okunevitch, A. I. 1969. Phys. Lett. $\underline{29A}$, 239.

VITA AUCTORIS

I was born on September 4, 1944 in Lublin, Poland.
After graduating in 1962 from a high school in Poznań,
Poland, I began my physics studies at the University of
Poznań. In 1964, I transferred to the Jagiellonian
University in Kraków where, in 1968, I obtained the degree
of Master of Science in physics. From 1968 to 1969 I was
a research assistant at the Institute of Nuclear Physics
in Kraków and, in 1969, I registered in the Faculty of
Graduate Studies at the University of Windsor.